ELSEVIER

Coordination Chemistry Reviews 162 (1997)
345–415

COORDINATION CHEMISTRY REVIEWS

Iron 1994

Ebbe Nordlander, Jacqueline G.M. Nairn, Anders Thapper, Christian Lorber, Teresa Mlodnicka

Contents

PII S0010-8545(96)01334-3

1. Introduction

This review covers the coordination chemistry of iron for 1994. The following journals have been covered by a combination of searching in *Chemical Abstracts* and independent searches in the following journals: *Acta Chem. Scand.*; *Acta Crystallogr., Sect. C*; *Angew. Chem., Int. Ed. Eng.*; *Chem. Ber.*; *Gazz. Chim. Ital.*; *Helv. Chim. Acta*; *Inorg. Chem.*; *Inorg. Chim. Acta*; *J. Am. Chem. Soc.*; *J. Chem. Soc., Chem. Commun.*; *J. Chem. Soc., Dalton Trans.*; *J. Coord. Chem. J. Mol. Catal.*; *Mendeleev Commun.*; *New J. Chem.*; *Polyhedron.*

Carbonyl compounds have been classified as organometallic compounds and are not included. Most iron-heterometal complexes have been excluded. This review does not aim to be fully comprehensive; omissions or errors are entirely the fault of the authors.

2. Complexes with hydrogen or hydride ligands

Mössbauer spectroscopy has been used to investigate the relative importance of σ- and π-effects in dihydrogen coordination in two complexes, *trans*-$[Fe(H_2)H(dppe)_2]BF_4$ and *trans*-$[Fe(H_2)H(depe)_2]BF_4$ (depe = $Et_2PCH_2CH_2PEt_2$) [1]. The studies show that H_2 is a very weak σ-donor and a strong π-acid ligand in these complexes; π-bonding is more important for H_2 than for a CO or a N_2 ligand in corresponding complexes. The H-H bond lengthens compared to H_2 in the gas phase but does not break. This is explained by the stability of the octahedral Fe(II) geometry compared to the seven-coordinate Fe(IV) complex that would be the result of the bond breaking.

Treatment of the hydrides $[FeH(H_2)L_4]^+$ (L = $P(OEt)_3$ or $PPh(OEt)_2$) with the appropriate heteroallenes CS_2, RNCS and PhNCO leads to the preparation of dithioformato $[Fe(S_2CH)L_4]^+$, thioformamido $[Fe(RN=CH=S)L_4]^+$ (R = Et, *p*-MeC_6H_4) species as well as $[Fe(PhN=C=O)L_4]^+$. Substitution with CO and isocyanides was achieved, giving $[Fe(RN=CH=S)(CO)L_3]^+$, $[Fe(RN=CH=S)(p\text{-}MeC_6H_4NC)L_3]^+$, $[Fe(PhN=C=O)(CO)\{P(OEt)_3\}_3]^+$ and $[Fe(p\text{-}MeC_6H_4NC)L_3]^+$ [2].

The dihydrogen complex *trans*-$[FeH(H_2)L]^+$ (**1**; L = *meso*-tetraphos-1, *R,S*-$Ph_2PCH_2CH_2P(Ph)CH_2CH_2P(Ph)CH_2CH_2PPh_2$) has been synthesised by reac-

tion of HBF_4 with *trans* $M(H)_2L$, which contains inequivalent *trans*-hydrides. The H-H distance in the rapidly spinning dihydrogen ligand has been calculated from T_1(min) data to be 0.88 Å. No intramolecular H atom exchange was observed for (**1**) [3].

3. Complexes with cyanide and other pseudo-halide ligands

Three complexes of the type $Na_3[Fe(CN)_5(L)]$ (L = 1,4-thioxane (**2**), 1,4-dithiane (**3**) and 1,3-dithiane (**4**)) have been prepared and spectroscopically characterized [4]. IR measurements indicate that the ligands are coordinated to the pentacyanoferrate(II) ion through the S atoms. The σ-donor and π-acceptor properties of the ligands were analysed from Mössbauer parameters, isomers shifts and quadropole splitting. The ligands were found to be poor σ-donors but good π-acceptors. The kinetics of ligand exchange were studied using pyridine as an entering ligand. A dissociative mechanism is proposed based on the existence of a rate saturation, the rate constants for dissociation being 5.7×10^{-4} s^{-1}, 5.6×10^{-4} s^{-1} and 3.4×10^{-4} s^{-1} for (**2**), (**3**) and (**4**), respectively.

4. Complexes with nitrogen donor ligands

4.1. Complexes with N-heterocyclic ligands

4.1.1. Complexes with pyridine and polypyridine ligands

Ligand-driven light-induced spin changes have been obtained by utilizing *cis-trans* photoisomerizable ligands. For spin conversion to function, at least one of the two compounds must have a thermally induced spin crossover. A *cis-trans* pair fulfilling these demands, *viz.* $[FeL_4(NCS)_2]$ (L = *trans*-4-styrylpyridine (**5**) and *cis*-4-styrylpyridine (**6**)), has been synthesized and the crystal structures of (**5**) and (**6**) have been determined. Their core have the same geometry with the SCN^- ligands in *trans* position. Complex (**5**) has a thermally induced $S=2 \leftrightarrow S=0$ crossover centred around 108 K while (**6**) remains in its high-spin state down to 4.2 K. The highest temperature for the experiment to function is 90 K but at this temperature the quantum yield is very low due to rigidity in the solvent [5].

The synthesis of the new hexadentate nitrogen ligand (**7**) and the synthesis and crystal structure of complexes of (**7**) with Fe(II)/(III) have been reported. Iron(II) gives the mononuclear $[M(7)]^{2+}$ (**8**). For the perchlorate salt, the structure around the iron(II) is *pseudo*-octahedral with pyridine nitrogen atoms *cis* and *trans* to the amine nitrogen atoms. Iron(III) gives the tetranuclear $\{[Fe_2(\mu\text{-}O)(\mu\text{-}OAc)_2]_2(\mu\text{-}bpteta)_2\}(ClO_4)_4$ and its structure can be described as a dimer of dimers with two $N_3Fe(\mu\text{-}O)(\mu\text{-}OAc)_2FeN_3$ cores spanned by the ligands. The tetranuclear complex shows a strong antiferromagnetic exchange coupling ($J = -120\ cm^{-1}$). The mononuclear complexes shows a *quasi*-reversible oxidation corresponding to the M(II)↔M(III) process [6].

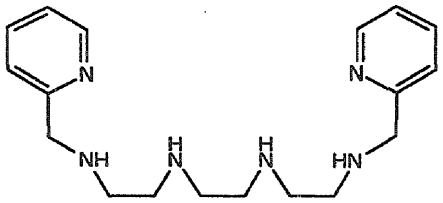

(7)

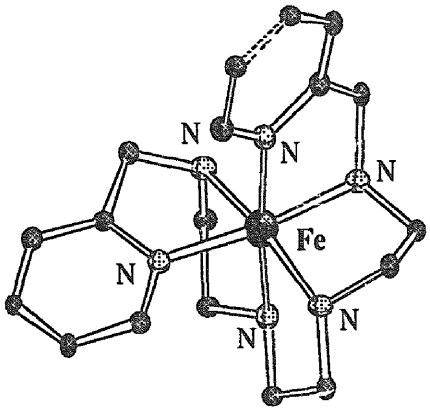

(8)

The dehydrogenation of amines appears to be dependent on coordination geometry. The two geometrical isomers, *mer*- and *fac*-tricyano[(**9**)]ferrate(II) give the iron(II) complex with dehydrogenated ligand and iron(III) complex with intact ligand, respectively, upon oxidation with $(NH_4)_2SO_4$ or H_2O_2 at neutral pH [7]. The reaction of iron(II) perchlorate with (2-pyridyl)bis(2-pyridylamino)methane (**10**) in the presence of air includes a metal-assisted deamination/oxidation during the complexation to give $[Fe(\mathbf{9})_2]ClO_4$ (**11**). The crystal structure of (**11**) shows that the ligand sphere around the iron centre is *pseudo*-octahedral. Measurements of the magnetic moments suggest a low spin d^5 configuration for the iron complex. The iron complex also exhibits a *quasi*-reversible or reversible oxidation assigned as the Fe(III)↔Fe(IV) redox process [8].

4.1.2. Complexes with other N-heterocyclic ligands

The synthesis and characterization of a dinuclear iron(III) complex $[ClFe(\mathbf{12})FeCl_3]\cdot 3H_2O$, has been studied by elemental analysis, EPR and ^{1}H-NMR spectroscopic, Mössbauer and magnetic susceptibility measurements [9]. Variable-temperature magnetic susceptibility in the temperature range of $80 < T < 300$ K was least squares fitted, with $J = -7.0$ cm^{-1}, supporting weak exchange coupling between iron atoms. Mössbauer data support the presence of distinct coordination environments for the two iron atoms.

Reaction of triisopropyl-TACN (**13**) or triisobutyl-TACN (**14**) with $FeCl_3\cdot 6H_2O$ in protic media does not result in complex formation. Instead, the macrocycles are singly protonated and the iron is incorporated into the anion, either as $[FeCl_4]^-$ or $[Fe_2OCl_6]^{2-}$. The fact that ligands (**13**) and (**14**) do not chelate iron is attributed to steric effects.

The crystal structure of $[\mathbf{13}\cdot H][FeCl_4]^-$ and $[\mathbf{14}\cdot H][Fe_2OCl_6]$ have been determined [10]. Furthermore, the potentially hexadentate ligand 1,4,7-tris(pyrazol-

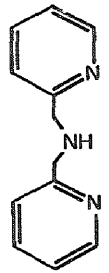

(9)

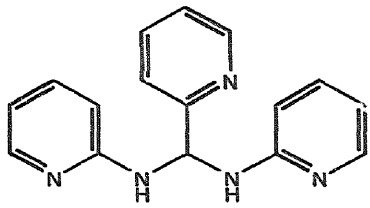

(10)

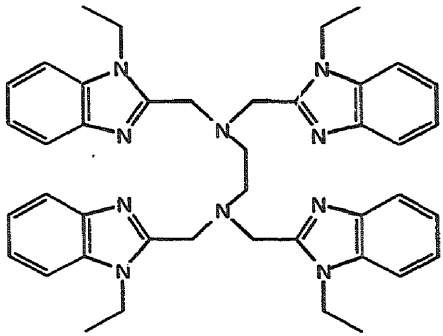

(12)

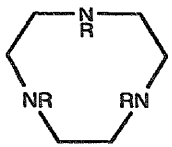

R=^{i}Pr (13)
^{i}Bu (14)

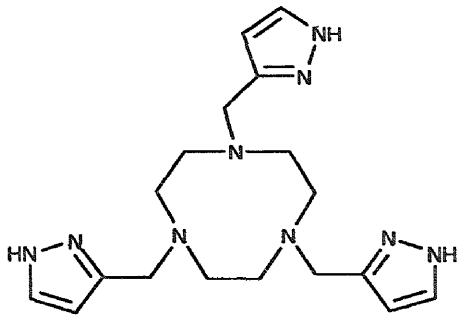

(15)

3-ylmethyl)-TACN (15) has been synthesized. The protonated form 15 · 6HCl reacted with iron perchlorate to give [Fe(15)][ClO_4]$_3$ [11].

A series of monomeric carboxylate ferrous complexes with the tripodal N_3 ligand

$[HB(3,5\text{-}iPr_2pz)_3]^-$ (**16**) has been synthesised and characterised in order to model the iron site in non-heme iron proteins which bind or activate dioxygen [12]. The X-ray structures of [Fe(OAc)(**16**)] (**17**), [Fe(OBz)(MeCN)(**16**)] (**18**) and [Fe(OOC^{t}Bu)(**16**)] (**19**) are reported. The five-coordinate complex [Fe(OBz)(**16**)] (**20**) was found to bind a variety of σ-donating ligands such as dimethyl sulfoxide and pyridine. The reaction between these ferrous compounds and dioxygen has been explored. Compound (**20**) was found to bind dioxygen to form an adduct that is reasonably stable below -20°C. Results identified the adduct as a μ-peroxo dinuclear ferric complex. Above -20°C, irreversible oxidation occurred, resulting in the formation of the trimeric ferric complex [(**16**)$Fe(OBz)_2(O)Fe(OH)(OBz)_2$Fe(**16**)].

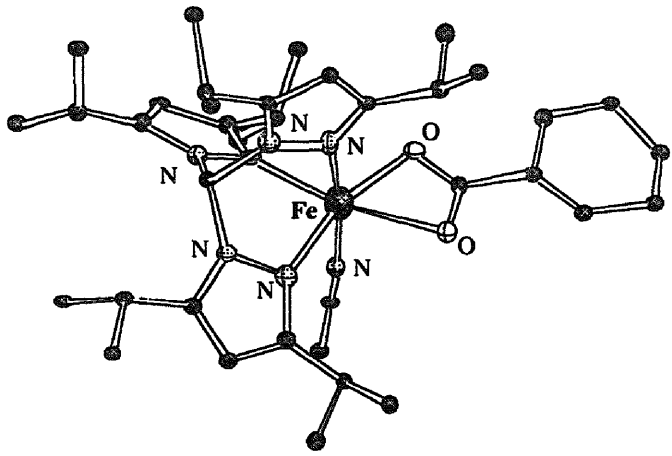

(**18**)

Two iron(II) compounds, $[Fe_3(\mathbf{21})_8(H_2O)_4](BF_4)_6$ (**22**) and $[Fe_3(\mathbf{21})_6(H_2O)_6](tos)_6$ (**23**) (tos = tosylate) have been synthesised by the reaction of iron(II) salts and the triazole ligand (**21**). The crystal structures of (**22**) and (**23**) have been solved and consist of three iron(II) centres in a linear arrangement with three bridging triazole ligands connecting the central iron atom with each of the two other. The dihedral angle between triazole and phenyl rings of the bridging ligands is 71.4° in (**21**) and 33.2° in (**23**). Heating (**23**) to 100°C gives $[Fe_3(\mathbf{21})_6(H_2O)_3](tos)_6$ (**24**). Magnetic measurements showed that the three iron(II) centres in (**22**) are high-spin in the temperature range investigated while (**23**)·$4H_2O$ and (**24**) undergo a gradual spin-conversion centred at $T_{1/2} = 245$ and 330 K, respectively. This is attributed to the difference in the dihedral angle in the bridging ligands [13].

The effect on the spin-crossover behaviour of $[Fe(\mathbf{25})_2(NCS)_2]\cdot H_2O$ [(**25**) = 4,4′-bis(1,2,4-triazole)] when metal dilution is made in the mixed-crystal series $[Fe_xM_{1-x}(btr)_2(NCS)_2]\cdot H_2O$ (M = Ni or Co) has been studied. When Fe(II) is diluted with Ni and x changes from 1.00 to 0.26, the transition temperature varies

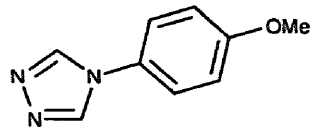

(21)

from 121 to 132 K in the cooling mode and from 145 to 132 K in the heating mode. When cobalt is used for diluting changing x from 1.00 to 0.23, the transition temperature decreases from 121 to 98 K in the cooling mode and from 145 to 98 K in the heating mode. The hysteresis vanishes for $x \approx 0.37$. The enthalpy and entropy change for spin conversion of iron(II) mononuclear complex decreases in both cases. Differences are found for how the transition temperatures and the hysteresis width changes with x as well as the existence of a residual high-spin fraction at low temperatures in the $[Fe_xCo_{1-x}]$ series [14,15].

Two solvates of $[Fe(\mathbf{26})_2(NCS)_2] \cdot n CH_3CN$ with $n = 1$ (**27**) and $n = 1/2$ (**28**), have been synthesised and their crystal structures have been determined. Complex (**27**) shows a high-spin↔low-spin conversion in the temperature range from 110 to 280 K while complex (**28**) is paramagnetic from 4.2 to 290 K. The crystal structure of (**27**) has been determined at 135 and 290 K. The room temperature and low temperature structures of (**27**) are very similar with iron atoms lying in a distorted octahedron with NCS^- ligands in *cis*-position. Differences in the Fe-L distances and trigonal distortion in (**27**) could account for the different behaviours. In the low temperature structure of (**27**) the Fe-N(**26**) and Fe-N(CS) distances decrease and the FeN_6 core becomes more regular through modification of the trigonal distortion and large changes in the N-Fe-N angles. The gradual temperature dependence is proposed to reflect a Boltzmann distribution of a ${}^4A_1 \leftrightarrow {}^5T_2$ spin equilibrium [16].

4.2. Complexes with imines and oximes

The compound $[FeCl_2(\text{H-}\mathbf{29})_2]$ (**30**) is formed by the reaction of $FeCl_2$ with *N,N'*-diphenylformamidine (**29**). Reaction of (**30**) with methyllithium produces an unidentified, highly paramagnetic orange solid, possibly $[FeCl_2(\mathbf{29})_2]^{2-}$. Extraction of the orange solid into a thf/toluene mixture followed by addition of hexanes leads to the formation of $[Fe_2(\mathbf{29})_4]$ (**31**) whose crystal structure has been determined. Compound **31** is of the well-known lantern type but the arrangement of the bridging ligands is distorted compared to previously known related structures whose symmetries closely approximate or equal D_{4h}. The formamidinato ligands form asymmetrical bridges with one long and one short Fe-N distance; two of the bridges are pulled towards one iron centre while the other two are pulled towards the other iron atom. The Fe-Fe bond length is 2.462(2) Å.

Reaction of (**30**) with butyllithium in thf leads to the formation of $[Fe_2(\mathbf{29})_3]$ (**32**) whose crystal structure has been determined. Compound (**32**) contains a mixed-

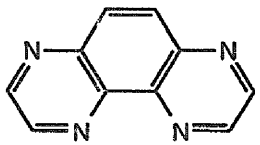

(26)

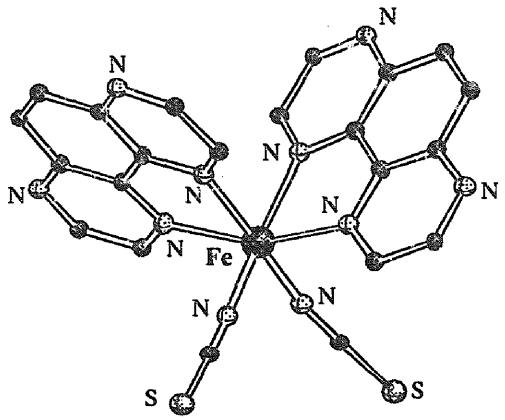

(27)

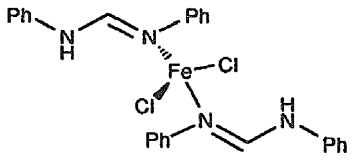

(30)

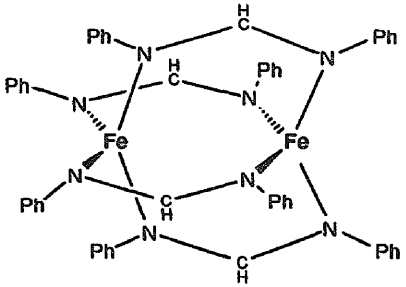

(31)

valent dinuclear iron unit bridged by three formamidinato groups. The Fe-Fe bond distance is short, 2.2318(8) Å. The EPR spectrum of (32) in a toluene glass (10 K) shows two signals at $g=1.99$ and 7.94 [17,18].

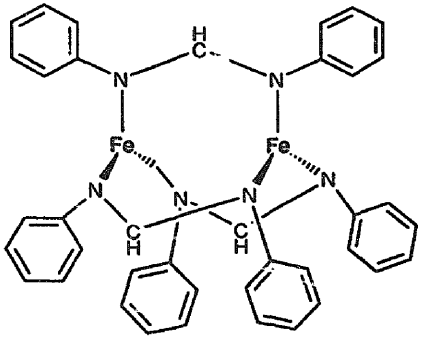

(32)

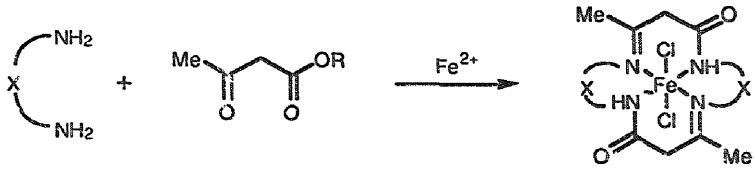

X= -$(CH_2)_2$-, R=Me (33), Et (34);
X= -$(CH_2)_3$-, R=Me (35), Et (36)
X=-C_6H_4-, R=Me (37), Et (38)

4.3. *Complexes with macrocyclic ligands*

A series of iron(II) complexes containing the tetraazamacrocyclic ligands (33)-(38) have been prepared by the condensation of 1,2-diaminoethane, 1,3-diaminopropane and *ortho*-phenylene diamine with methyl acetoacetate or ethyl acetoacetate in the presence of $FeCl_2 \cdot 6H_2O$ at room temperature [19]. The structure and bonding of the macrocyclic ligand complexes have been studied by elemental analysis, magnetic susceptibility measurements, IR and ^1H NMR spectroscopies, mass spectrometry, and their EPR and electronic spectra. The stereochemistry around the metal ion is octahedral with four of the coordination sites being occupied by the nitrogen atoms of the macrocyclic ligand and the remaining octahedral positions being occupied by two chlorine atoms.

Magnetic, UV-VIS spectroscopic and NMR measurements on a series of Werner complexes containing iron(II) encapsulated by the hexaamine ligands (39)-(41) have been performed over a range of temperatures. Encapsulation of the transition metal ion by these sarcophagine ligands permits its electronic and spectroscopic properties to be studied in a magnetically dilute and kinetically inert environment. The saturated nature of the amine yields a cryptand of the innocent kind so that the ligand field absorption of the metal containing cages is not obscured by intense charge transfer bands. High-spin and low-spin isomers were found to coexist in solution and the temperature dependence of the physical parameters is characteristic of a spin equilibrium between molecular states of $^1A_{1g}$ and $^5T_{2g}$ origin [20].

The bis-macrocyclic Fe(II)/Fe(II) complex (42) has been investigated by optical and Mössbauer spectroscopy as well as cyclic voltammetry. The Mössbauer spectrum indicates that the tetraiminoethylene dimacrocycle is a very good π-acceptor. Electrochemical oxidation results in the formation of the mixed-valence Fe(II)/Fe(III) complex (43).

A large solvent dependence that is thought to come from axial ligand exchange by coordinating solvent molecules indicates that the oxidation occurs at the metal centre. The Mössbauer spectrum of (43) shows that the two iron atoms are equivalent. Cyclic voltammetry of (43) in dry acetonitrile shows two reversible oxidations separated by 500 mV and it is suggested that (43) is a valence-averaged class III complex stabilized by delocalization. Electrochemical reduction of (43) formally

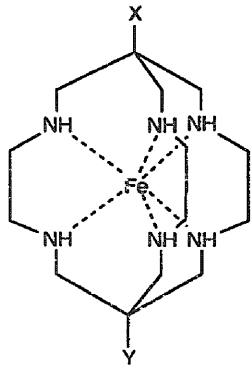

(39): X=Y=H; (40): X=Y=NH_2; (41): X=Y=NH_3

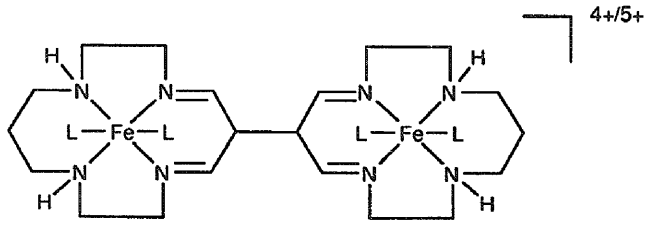

(42), (43) (L = solvate)

occurs at the ligand but a large solvent dependence and a shift in the first reduction potential upon exchange of Fe for Ni indicates mixing of orbitals [21,22].

The conformationally flexible macrocyclic iron(II) complex (44) has been synthesized. The complex converts easily between C_{2h} and C_{2v} conformations which moves the boron-linked phenyl groups into or out of contact with bound substrates. The π-π interactions between the phenyl groups and bound substrates are dominated by Coulombic forces and span 8 kcal mol^{-1} in energy from attractive (charge transfer) to repulsive. The π-π interactions add to or subtract from the stronger metal-ligand bonding interactions giving net effects up to six orders of magnitude on substrate-binding equilibria and dissociation rates [23].

An Fe(III)N_4O_2 chromophore has been crystallographically characterized for the first time. The Fe-N and Fe-O(CO) distances are 2.014(7) and 1.925(5) Å, respectively. The chromophore is a part of a one dimensional polymer that is formed from a *trans*-[Fe(III)(cyclam)][{$Fc(CO_2)_2$}$_2$H] ([$Fc(CO_2)_2$]$^{2-}$ = 1,1′-ferrocenedicarboxylate) by strict self-assembly via Fe(III)-carboxylate covalent bonds and hydrogen bis-carboxylate hydrogen bonds [24].

4.4. Miscellaneous N-donor complexes

Cationic complexes with a series of tridentate ligands L, [FeL_2][ClO_4]$_2$ (X=H (45), OH (46), or Cl (47)), have been isolated and characterized. The ligands were

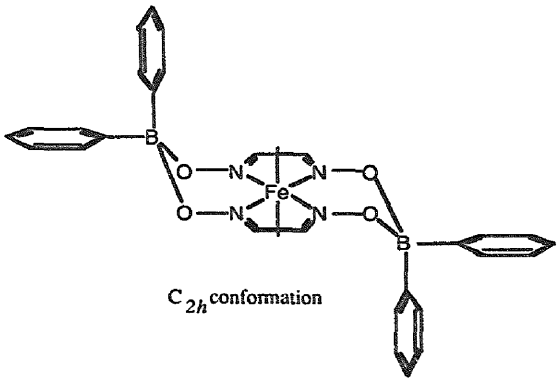

C_{2h} conformation

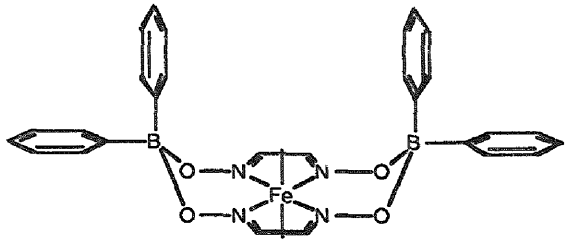

C_{2v} conformation

(44)

synthesized via condensation of *o*-phenylenediamine with 4-substituted pyridine-2,6-dicarboxylic acids. The $[FeL_2]^{2+}$ species show thermally induced spin-crossover behaviour ($^1A_1 \rightarrow {}^5T_{2g}$). This solution behaviour is most pronounced for X=H and is strongly diminished by electron-withdrawing substituents in the 4-position on the pyridine, leading eventually to pure high-spin states at room temperature in methanol. This suggests, in accord with ligand-field parameters evaluated from the analogous Ni(II) complexes, that - despite the strong electron-withdrawing properties of the substituents - the ligand-field splitting in the substituted $[FeL_2]^{2+}$ species must be lower than that in the unsubstituted species [25].

A spin crossover complex, $[Fe(\mathbf{48})_2](BF_4)_2$, has been investigated. In the temperature region between 160-185 K the complex shows a complete high spin-low spin transition ($^5T_2 \Leftrightarrow {}^1A_1$). The complex also shows the light-induced excited spin state trapping (LIESST) and reverse LIESST effect at low temperatures. The metastable HS state can be trapped by rapid cooling of the sample. The HS→LS relaxation monitored by Mössbauer spectroscopy shows strong deviation from first order kinetics [26].

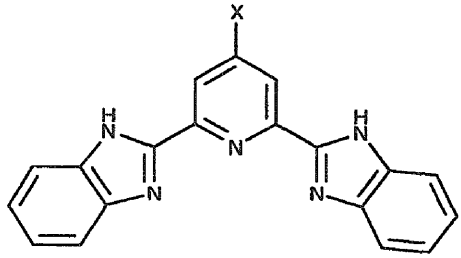

X = H (45), OH (46), Cl (47)

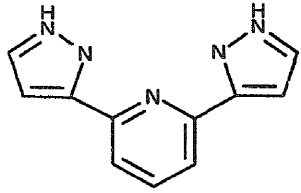

(48)

The iron complexes of two designed ligands, (49) and (50), have been reported. The complexes mimic the metal chelating potion of the anti-tumour drug bleomycin. After reaction with O_2 they give low-spin hydroperoxo Fe(III) species with EPR spectra that are similar to that of activated bleomycin. They also, like bleomycin, induce DNA damage via an oxidative pathway and promote oxo-transfer to olefinic substrates. The O_2 activation capacity of the two new complexes are identical. This excludes the possibility that the secondary amine group in ligand (49) assists the O_2 activation process by internal hydrogen bonding. It is suggested that this also is true for bleomycin [27].

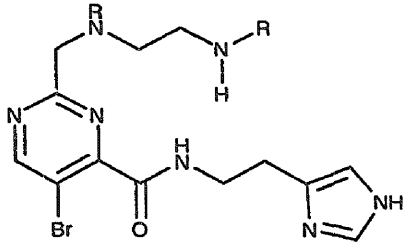

R= H (49) or Me (50)

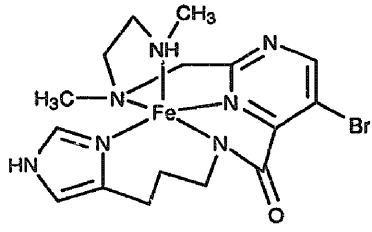

[Fe(II)(50)]+

The iron(IV) complex [(51)FeCN] (52) has been synthesized. The complex was made by adding NaCN to a solution of [Fe(51)] giving [(51)FeCN]- that was subsequently oxidized by adding ferrocenium triflate. Both NMR and IR spectro-

scopy indicate that the cyanide ligand is present in (52). The Mössbauer spectrum of (52) revealed a small and negative isomer shift which is indicative of an iron(IV) complex. The complex has a low-spin configuration unlike [Fe(51)] which has a high-spin configuration [28].

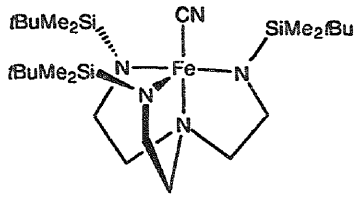

(52)

5. Complexes with tetrapyrrole macrocycles

5.1. Complexes with phthalocyanines

The absorption and magnetic circular dichroism spectra of iron(II) phthalocyanine complexes with varying axial ligands $[L_2Fe(II)Pc]^{2-}$ have been assigned. The axial ligands L were imidazole, *N*-methylimidazole, pyridine, methylpyridine, piperidine, ammonia, cyanide, and carbon monoxide. The complexes could be divided into three classes on the basis of their spectral features due to the strength of their σ and π interactions, (i) strong σ donors-weak π acceptors [L=im, Meim, py, Mepy, pip and NH_3], (ii) weak σ donors-strong π acceptors [L=CO], and (iii) strong σ donors-weak π donors [$L=CN^-$] [29].

5.2. Complexes with porphyrins

5.2.1. Axially ligated porphyrin complexes

The complex [Fe(TPP)Cl] (53) and its trivalent Mn and Co analogues have been found to be mild as well as efficient stereo- and regio-selective catalysts for the synthesis of lactam from *N*-phenyl-spirooxaziridine [30]. Complex (53) has also been found to catalyse hydrogenation of various α,β-unsaturated esters by $NaBH_4$ in tetrahydrofuran-methanol solutions. High turnovers are found for reactions carried out at 30°C under nitrogen. α,β-Disubstituted esters are hydrogenated rapidly whereas β-substituted are hydrogenated very slowly. The highest turnover number of 4580 per hour is obtained for ethyl-2-methylbut-2-enoate. Deuterium labelling studies show that H^- of $NaBH_4$ and H^+ from methanol add to the β- and α-carbons of the double bond. UV-VIS, ^1H NMR and EPR spectroscopies indicate that hydrogenation proceeds via an iron(II) intermediate [25]. Furthermore, (53) catalyses electrochemical reduction of CO_2 at the Fe(I)/Fe(0) redox wave in DMF.

Carbon monoxide is the only product. In the presence of the weak Brønsted acid 2-trifluoroethanol, the catalytic efficiency reaches the unprecedented value of 131 [31].

The complex [Fe(III)(TMP)Cl] and (**53**) as well as its μ-oxo dimer have been used for photocatalytic oxygenation of several alkenes with dioxygen. The product composition depends on the nature of the substrate and its concentration. Alkenes with strained double bonds such as norbornene, α-pinene, 1,5-*cis*,*trans*-cyclodecadiene and cyclooctene give preferentially epoxides whereas mainly allylic oxygenation is observed for cyclohexene, cyclopentene and cycloheptene. It is proposed that the photolytically generated porphyrin-Fe(IV)=O complexes are the catalytically active species. The enantio, regio-, and chemoselectivities of the photooxygenation are explained in terms of abstraction of an allylic hydrogen atom, catalysed autoxidation and direct oxygen-transfer reactions [32].

The nitrobenzene derivatives *p*-X-$C_6H_4NO_2$ (X=MeO, Me, H, Cl, F_3C) are efficiently reduced by a mixture of (**53**) and $NaBH_4$ in such solvents as diglyme, diglyme-methanol and tetrahydrofuran-methanol. The six-electron reduction of nitrobenzene to aniline is accomplished. Substrate conversion and yields of products increase when the electron-withdrawing character of the substituents is augmented. The catalytic reduction proceeds through nitrosobenzene and phenylhydrazine. Electron paramagnetic resonance and UV-VIS spectroscopies indicate that [Fe(II)TPP] is the putative active species. The presence of a protic solvent accelerates the reduction of the nitrobenzene derivatives with electron-donating groups and disfavours the reaction when the electron-withdrawing groups are present [33].

The oxidation and reduction potentials of iron(III) β-substituted porphyrins of the formula [Fe(III)(Br_xTPP)Cl] (x=1-8) have been measured as a function of the number of Br substituents varying systematically between 0 and 8. It has been found that each complex undergoes two reversible one-electron oxidations and three one-electron reductions in benzonitrile. The half-wave potentials of the first reduction steps vary linearly with the number of the bromine substituent and are shifted in a positive direction by 51 mV per each Br atom. In contrast, the half-wave potentials for oxidation are shifted in positive direction only for x=0-3 after which negative shift are observed which means that Fe(Br_8TPP)Cl is more easily oxidized than Fe(TPP)Cl. This effect is attributed to the increasing distortion of the macrocycle caused by additional bulky substituents, which dominate the inductive effects of the halogens and decrease stability of the HOMO level making the oxidation easier [34].

The perhalogenated porphyrin complex (**54**), which is water soluble, is an efficient catalyst for the oxidation of hydrocarbons [35]. It gives particularly good results in the oxidation of aromatic rings. The complex [Fe(TFPPBr_8)Cl] carrying 20 fluorine substituents at the four phenyl rings and 8 bromine substituents at the pyrrolic positions, which is an effective catalyst of the oxidation reactions, has also appeared exceptionally active catalyst for the hydroperoxide decomposition [36]. It is suggested that the most common mechanism for the hydrocarbon oxidation is radical-chain autoxidation in which radicals are generated by oxidation and reduction of alkylhydroperoxides.

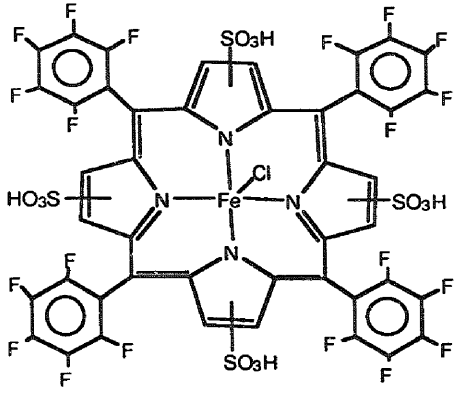

(54)

A low-spin $[Fe(III)(TPP)(4\text{-}CNPy)_2]ClO_4$ complex has been synthesised and characterized by X-ray, Mössbauer and EPR measurements [37]. All properties are consistent with strong π-accepting properties of the axial ligands which have relative perpendicular orientation. The porphyrin core is strongly ruffled and leads to extremely short Fe-N_{por} bond distances of 1.952(7) Å. The axial Fe-N bond distance is 2.002(8) Å. The ruffling is attributed to electronic rather than steric factors. Mössbauer and EPR spectra are consistent with an iron(III) ion that has unusual ground-state configuration $(d_{xz}, d_{yz})^4(d_{xy})^1$.

Crystal structures of the high spin azide complex $[Fe(III)(TPP)N_3]$ (**55**) and of its six-coordinate low spin adducts $[Fe(III)(TPP)N_3L]$ (L = 1-methylimidazole, 1,2-dimethylimidazole) have been determined. In all these complexes the azide ligand is bonded in a bent fashion with Fe-N-N angle of 122°. In $[Fe(TPP)N_3]$, the porphyrin core is domed and the iron is displaced 0.510 Å from the porphyrin core and 0.457 Å from the plane of the four pyrrole nitrogens. In the two six-coordinate derivatives the porphyrin core is ruffled with the methane carbons alternating above and below the mean plane of the core with an average displacement of 0.15 Å in the 1-MeIm and 0.36 Å in 1,2-Me_2Im. The iron atom is projected slightly toward the azide in the former and is located in the core in the latter. However, in 1,2-Me_2Im steric congestion is manifested by an increase in the Fe-N_{Im} bond distance of 0.083 Å and tipping of the imidazole ligand by 15° from the symmetrical position observed in 1-MeIm derivative [38].

The distribution of unpaired electron density within the porphyrin π orbitals of two unsymmetrically substituted derivatives of iron(III) tetraphenylporphyrin, $[(p\text{-}Cl)(p\text{-}NEt_2)_3(TPP)Fe(N\text{-}MeIm)_2]Cl$ and $[(p\text{-}NEt_2)(p\text{-}Cl)_3(TPP)Fe(N\text{-}MeIm)_2]Cl$ has been investigated by measuring ^1H COSY and NOESY spectra. The presence of an electron-withdrawing substituent at one of the phenyl rings involves spin delocalization to the π orbital with low electron density at the β-pyrrole carbons closest to and most distant from the unique substituent. In contrast, when a relatively electron-donating substituent is present at one of the phenyl rings the π

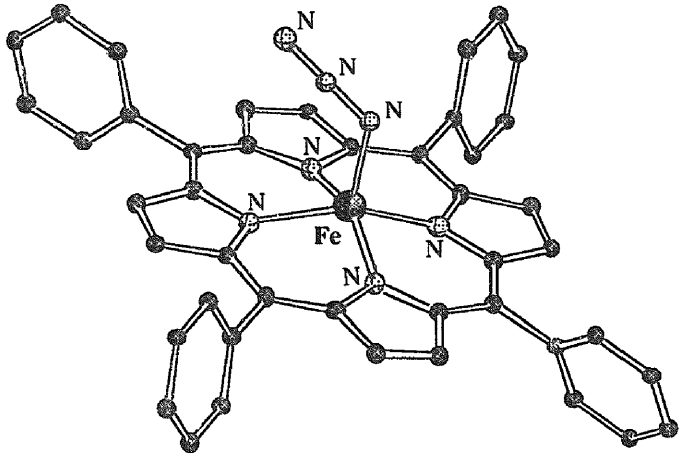

(55)

orbital preferred for spin delocalization is that with large electron density at the closest and most distant β-pyrrole carbons. Hückel molecular orbital calculations support these assignments [39].

Proton NMR, ^{13}C NMR and EPR spectral properties of a series of low-spin [(R-TPP)Fe(L)$_2$Cl] (R-TPP=*meso*-tetrakis-(2,4,6-R$_3$-phenyl)porphyrinato, R=H (**56**), Me (**57**), Et (**58**), Pr (**59**); L=2-alkyl- and benzimidazoles) have been investigated. The variable temperature ^1H NMR spectra show that the rotation of the axial ligands slows down on the NMR time scale at low temperatures to give four pyrrole signals. Carbon-13 NMR spectra of ^{13}C-enriched Fe(TMP)(2-methylimidazole)$_2$Cl at the *meso* positions give two *meso* signals of equal intensity below -25°C. These results indicate that the two axial ligands are perpendicularly aligned over the diagonal C_{meso}-Fe-C_{meso} axes. This unfavourable orientation of the ligands is attributed to the deformed structure of the porphyrin core in solution which is additionally confirmed by the relatively small slopes in Curie plots of the pyrrole-H and the *meso*-^{13}C signals. In the mixed ligand complexes having one hindered and one unhindered ligand, the rotation of the former becomes frozen. The activation free energies for rotation, determined by the dynamic NMR spectroscopic technique, change in the range of 11.3-13.6 kcal mol^{-1} depending on the bulkiness of the axial ligands and *o*-alkyl substituents [40].

The complex [Fe(III)(TPP)(OSO_2CF_3)] (**60**) in both monoclinic and triclinic phases has been structurally characterized by single crystal X-ray diffraction for the first time. Only one type of molecular site has been found in the monoclinic phase. The compound exhibits typical characteristics of a spin-admixed iron(III) porphyrin compound with a considerable amount of $S=5/2$ character in the ground state. The complex in the triclinic phase is the first pentacoordinate Fe(III)(P)X system which exhibits spin-state isomerism in the solid state with two crystallographically and

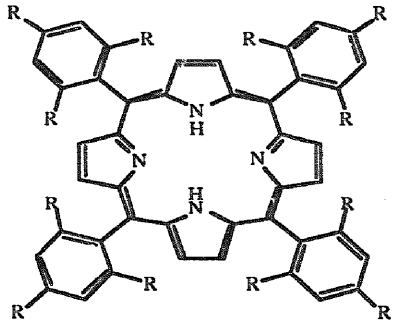

R = H (56), Me (57), Et (58), Pr (59)

magnetically distinct sites in the same unit cell. Crystal data for the complexes in the monoclinic phase at 293 K and triclinic phase at 293 and 188 K have been determined [41].

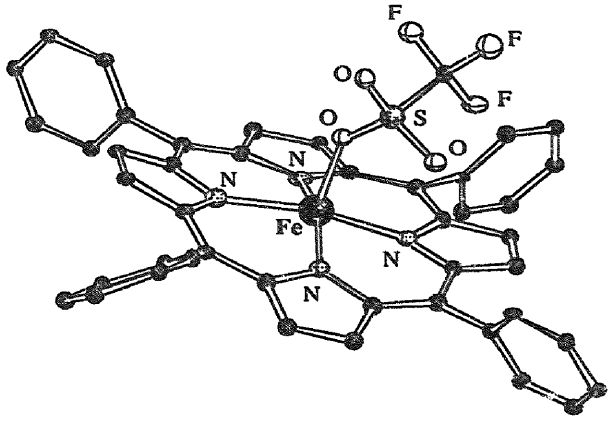

(60)

The complexes [Fe(61)Cl], and [Fe(62)Cl] have been used as catalysts for hydroxylation of cyclohexane in 1,2-dichloroethane solutions using iodosylbenzene as oxygen donor. The efficiencies of the catalysts were investigated not only in solution but also with the porphyrin complexes supported on imidazole propyl gel (IPG) or silica gel (SG). The best results were obtained for the solution system (65% yield of cyclohexanol). The IPG and SG systems afforded 25% and 15% yields, respectively. When the imidazole/Fe(TDCPP)Cl ratio in IPG is decreased, the yield increases to 60% [42].

The complex $[Fe(OEP)(H_2O)]ClO_4.2H_2O$ has been obtained by treatment of the μ-oxo iron(III) dimer $[Fe(OEP)]_2O$ with aqueous $HClO_4$. The $[Fe(OEP)H_2O]^+$ cation was characterized by UV-VIS, IR, EPR and Mössbauer spectroscopies,

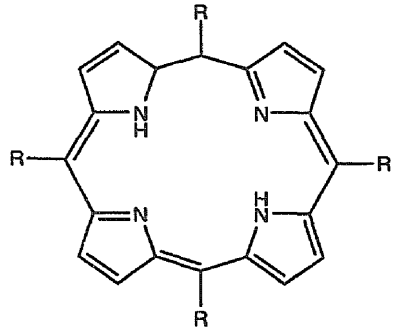

(61): R = 2,6-$Cl_2C_6H_3$; (62): R = C_6F_5

temperature dependent magnetic susceptibility measurements and a single-crystal X-ray structure. The average Fe-N_{por} distance is 1.982(4) Å, the axial Fe-O distance is 2.045(3) Å, and the iron atom is displaced of 0,20 Å from the 24 atom mean plane. These data are consistent with an admixed intermediate-spin state for iron(III) ($S=3/2,5/2$). The crystal structure of [Fe(OEP)(thf)$_2$]ClO_4 has also been determined [43].

Photochemical and photocatalytic behaviour of oxygenated solutions of [Fe(III)(**63**)Cl] (**63** = protoporphyrin IX) and [Fe(III)(OEP)Cl] in the presence of nitrogen ligands such as pyrazine (pyz) or pyridine has been investigated. Irradiation of these systems at $\lambda = 360$ nm induces oxidation of benzene to phenol, benzohydroquinones and quinones. Basic conditions (pH = 8-9), and a large excess of pyrazine with respect to the iron porphyrin, are required to effect photoreduction of Fe(III) porphyrin and hydroxylation of benzene. In neutral or acidic solutions a mixed-valence, polynuclear complex pyz-Fe(III)PP-pyz-Fe(II)P···Fe(II)PP-pyz-Fe(III)PP is generated in the presence of oxygen. The complex is stable in air for several days and is catalytically inactive [44].

5.2.2. Complexes with oxygen, peroxides and hydroxides

Geometrical parameters, Fe-O stretching frequencies and charge and spin densities for five-coordinate (porphyrinato)oxoiron(IV) complexes have been calculated using local density functional (LDF) theory. Two complexes, [(por)Fe=O] and [(por)Fe=O]$^+$ were chosen as models for peroxidase compounds II and I, respectively. In the optimized structure of (por)FeO, the Fe-O distance is 1.622 Å and the iron atom is located 0.215 Å above the N_4 plane. Realistic values of Fe-O stretching frequencies of 934 and 964 cm^{-1} are obtained for (por)FeO and [(por)FeO]$^+$ respectively. In both species two unpaired spins localized on the ferryl moiety are divided between Fe and O in the ratio 1.2:0.8. The third unpaired spin of [(por)FeO]$^+$ is distributed over the porphyrin ring as an a_{2u} cation radical [45]. Oxidation of perchloratoiron(III) *meso*-tetrakis(pentafluorophenyl)porphyrin, [Fe(III)(TFPP)(ClO_4)], by *meta*-chloroperoxybenzoic acid in dichloromethane solution at -80°C produces an oxoiron(IV) porphyrin cation radical as evidenced by low temperature UV-VIS, ^{1}H NMR and EPR spectroscopic measurements. A large

upfield shift for the pyrrole β-protons suggests that, unlike most *meso*-tetraarylporphyrin cation radicals which have been characterized as a_{2u} species, the $(TFPP^{+\cdot})Fe(IV)=O$ has a_{1u} character. The behaviour of $[Fe(III)(TFPP)]ClO_4$ complex is attributed to the low basicity of the perchlorate ion which itself is a weak ligand [46].

The preparation of [(TMP)Fe(IV)=O] has been accomplished via ligand metathesis of the stable Fe(III) porphyrin cation radical $[(TMP^{+\cdot})Fe(III)](ClO_4)_2$ over moist basic alumina. The cation radical has been obtained from the reaction of chloroiron(III) porphyrin (TMP)Fe(III)Cl with wet basic alumina followed by treatment with solid $Fe(ClO_4)_3$ in dichloromethane. The oxoiron(IV) porphyrin has also been generated by electrochemical oxidation of the corresponding hydroxoiron(III) porphyrin. The complex [(TMP)Fe(IV)=O], which is stable at room temperature in benzene, reacts readily with substituted styrenes affording aldehydes and epoxides but the selectivity is different from that observed for the corresponding cation radical [47]. The oxoiron(IV) complexes $[X\text{-}(TMP)Fe=O]^+(Cl^-)$, (X=H, I, Br_2, Br_4) (**64**)-(**67**) have been generated by oxidation of the corresponding Fe(III) porphyrins with *meta*-chloroperoxybenzoic acid. Temperature-dependent EPR and field-dependent Mössbauer measurements have revealed a strong ferromagnetic coupling between ferryl iron ($S=1$) and the porphyrin radical ($S=1/2$). Although halogen substitution at the β-pyrrolic positions causes distortion in the planarity of the porphyrin ring, it only leads to minor variations in zero-field splitting of the ferryl iron and in the ferromagnetic coupling between iron and porphyrin spin. This is consistent with the idea that the unpaired electron is in the a_{2u} orbital with increased spin density at the pyrrole nitrogens and the *meso* carbons [48].

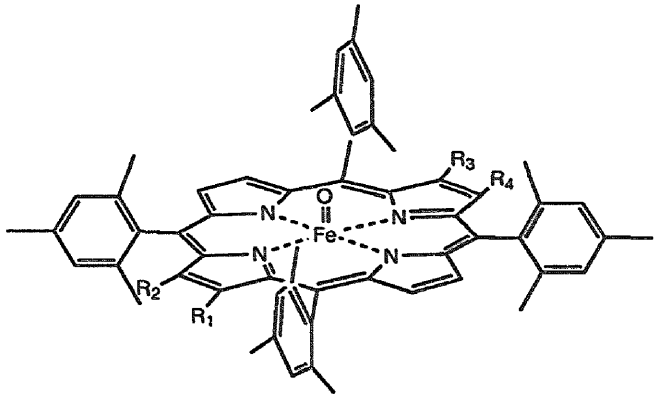

(**64**): R_1, R_2, R_3, R_4=H
(**65**): R_1=I, R_2, R_3, R_4=H
(**66**): R_1, R_2=Br, R_3, R_4=H
(**67**): R_1, R_2, R_3, R_4=Br

The effect of six axial ligands, *viz* -F, $HOCH_3$, -Cl, -OAc, $-OSO_2CF_3$ and $-OClO_3$ on the reactivity of the oxo-iron(IV)tetramesitylporphyrin cation radical $[(TMP^{+\cdot})Fe(IV)O]^+$ has been examined by EPR and ^1H NMR spectroscopies. The complexes were obtained by ozonolysis of the corresponding iron(III) porphyrins. Whereas the influence is small on the EPR spectra, the chemical shifts of the porphyrin protons depend considerably on the character of the axial ligand. A qualitative relation has been found between the field strengths of the ligands and the reactivity of the ferryl complexes [49].

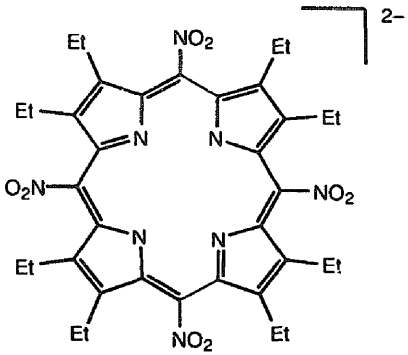

(68)

The μ-oxo dimer $[\{Fe(\mathbf{68})\}_2O]$ (**69**) has been synthesized by reacting NO_2 with [Fe(OEP)Cl] in dichloromethane under nitrogen at room temperature. The complex was characterized by ^1H NMR and IR spectroscopies. The introduction of NO_2 groups into the *meso*-positions of the octaethylporphyrin ligand increases the Fe(III)/Fe(II) reduction potential of the complex and its stability under oxidation conditions. The complex has been used as a catalyst for the liquid-phase oxidation of alkanes such as isobutane and propane by molecular oxygen. Turnovers up to 1680 were obtained for oxidation of isobutane at 80°C after 5 hours and the selectivity to isobutanol is 88%. Propane was oxidized with lower activity and selectivity [50].

5.2.3. Strapped porphyrin complexes

The superstructured basket handle porphyrins (**70**) and (**71**) have been derived from *meso*-tetraphenylporphyrin by linking two opposite phenyl rings in order to sterically protect both faces of the porphyrin macrocycle [51]. Fixation of the linking hydrocarbon arms to the phenyls is effected by either the amide (**70**) or ether (**71**) groups.

The interactions between the two Fe(III) basket-handle porphyrins and catechol (H_2cat) in dmso-water solution (80:20 v/v) in acidic and basic media have been investigated. A combined spectrophotometric and potentiometric study showed that in acidic media the 1-Hcat complex of 1:1 stoichiometry is obtained with the stability constant $\lg\beta = 8.6$ (25°C, 0.1 KNO_3). The relatively low value of the stability constant of this complex as compared with non-porphyrinic Fe(III) complexes with didentate

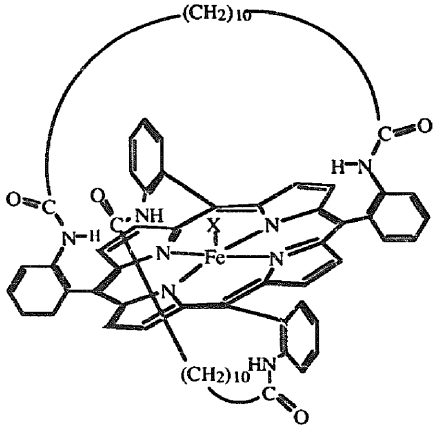

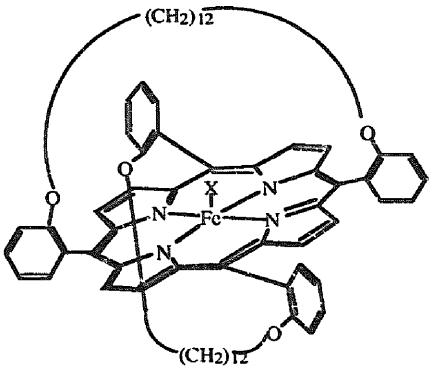

X= solv (H_2O or DMSO)

(70) (71)

catecholate ligands indicate monodentate binding of the hydrogenocatecholate anion imposed by the rigidity of the porphyrin macrocycle. In basic medium deprotonation of the hydrogenocatecholate complex is observed and the resulting catecholate complex with monodentate cat^{2-} anion is sensitive to oxidation by traces of dioxygen. The obtained results support the proposed substrate activation effected by the enzyme catechol 1,2-dioxygenase. There is no evidence for the formation of a 2-Hcat complex.

Five-coordinate [Fe(por)(L)] complexes, (por=(**72**), (**73**), (**74**); L= 1,5-dicyclohexylimidazole or 1,2-dimethylimidazole) reversibly bind O_2 and CO. The kinetics of the reactions have been investigated in toluene by spectrophotometric equilibrium titrations, stopped flow and laser flash photolysis. The absence of polarity effects in durene capped complexes is reflected by poor differentiation in binding of O_2 and CO. Only the derivative which is distorted due to a short linking chain discriminates between the two ligands and the effect is associated with large deformation of the porphyrin core from planarity [52].

Water-soluble "one face" hindered Fe(II) and Fe(III) porphyrin complexes have been obtained by sulfonation of basket handle porphyrin in concentrated sulfuric acid. The structural assignment of the porphyrins is based on ^1H NMR spectra of the free base. Anaerobic insertion of iron has been accomplished by reacting the free base porphyrin with iron(II) sulfate in water. As proved by EPR spectroscopy, the reaction affords pure monomeric *aqua*-iron(III) compound. The Fe(II) complex (**75**) has been obtained by reduction of the Fe(III) compound in water with an aqueous sodium dithionite solution under argon. Reaction of (**75**) with imidazole leads to the formation of a six-coordinate [Fe(II)(por)Im_2] complex [53].

The [Fe(II)TPP] derivatives (**76**)-(**79**), with variable degrees of distal steric hindrance provided by two lateral pivalamido pickets, have been investigated in the

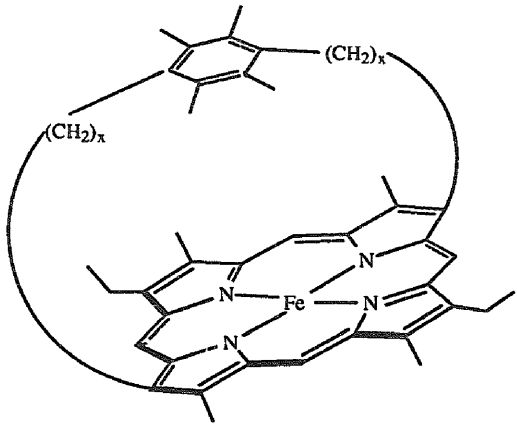

x = 4 (72), 5 (73), 7 (74)

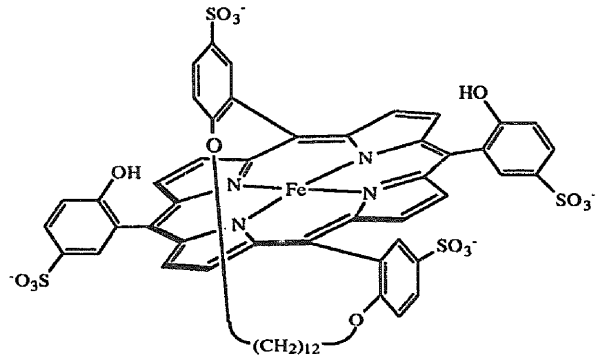

(75)

reaction of O_2 and CO binding. Upon increasing the steric hindrance, CO affinities decrease by 2-3 orders of magnitude while oxygen affinities become reduced only by a factor of 1.4-3.4, indicating a strong steric impediment vis-a-vis CO. The X-ray structure of two CO derivatives, and results derived from ligand rebinding kinetics using laser flash photolysis, prove that the steric interactions with CO involve a ruffling distortion of the porphyrin macrocycle and an expansion of the distal cavity rather than a putative bending of the Fe-C-O unit. The investigated system mimics the reactivity of oxygen-carrying hemoproteins [54].

Oxidation of the deformed iron(III) porphyrin complexes (**80**)-(**82**) with tris(*p*-bromophenyl)ammonium hexachloroantimonate affords iron(III) π-cation radicals as evidenced by UV-VIS, IR, ^{1}H NMR spectroscopies and magnetic susceptibility measurements which show antiferromagnetic coupling between Fe(III) spin (S= 5/2) and porphyrin cation radical spin (S= 1/2). A molecular mechanics simulation

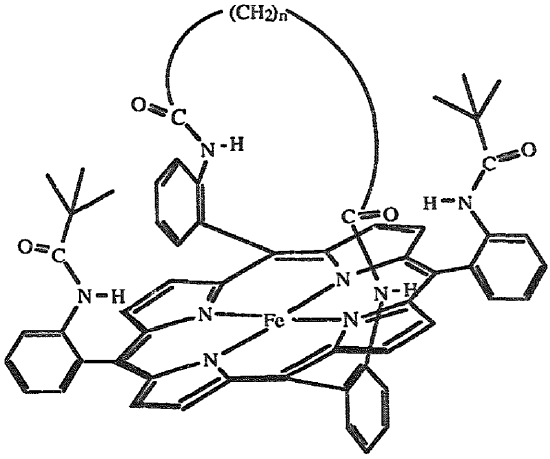

n=6 (76), 7 (77), 8 (78), 10 (79)

reveals deformation of the porphyrin core constrained by the covalently attached short bridging groups. The adjacent *trans* isomers show ruffled distortion while the adjacent *cis* isomers have saddle distortion [55].

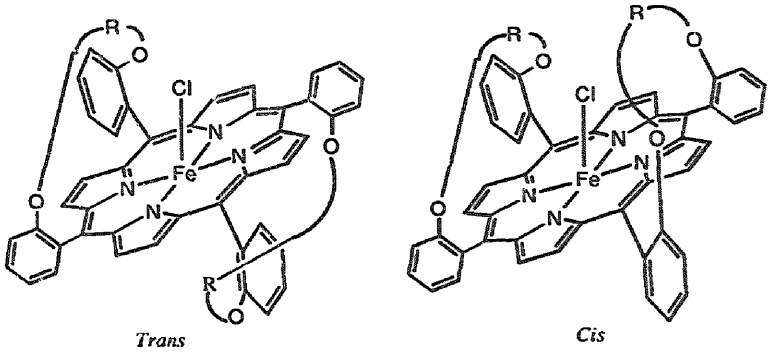

Trans *Cis*

R =

(80) (81) (82)

A series of iron(II) picnic-basket porphyrins (83)-(88) have been prepared [56]. In solution, the unhindered faces of the porphyrins are blocked by coordination of bulky imidazole derivatives and dioxygen is bound reversibly at room temperature within the cavity of the baskets. The oxygen affinities increase dramatically when

the basket size decreases. This effect is explained in terms of either dipole-dipole or H-bonding interactions between the terminally bound dioxygen and the amide protons of the linker arms. Proton NMR spectroscopy does not supply any evidence in favour of strong H-bonds within the pockets.

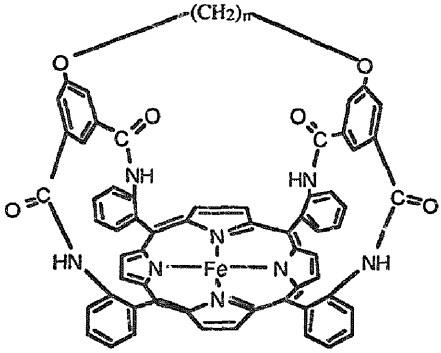

n = 2 (**83**), 4 (**84**), 6 (**85**), 8 (**86**), 10 (**87**)

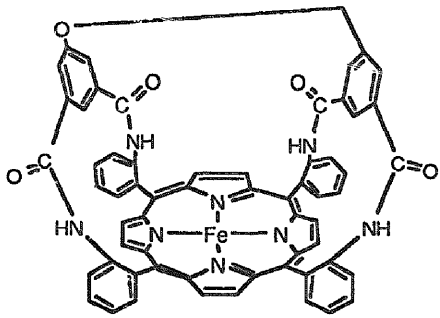

(**88**)

Resonance Raman (RR) spectra have been measured for CO adducts of the two sterically constrained iron(II) porphyrins (**89**) and (**90**). The C-O and Fe-C stretching frequencies indicate an increase in Fe→CO back bonding in (**89**) and decreased back bonding in (**90**) when compared with unconstrained porphyrins. These differences arise from the different polar environment of the bound CO molecule in the two adducts; in (**89**), close vicinity of the amide groups of the linker arms favours back bonding whereas in (**90**), CO interacts with the benzene π-cloud which restricts back bonding. Crystal structures of the investigated complexes show similar FeCO geometries with small amounts of bending and tilting up to *ca.* 10° each. It is concluded that polar interactions rather than Fe-C-O angular distortions determine the RR pattern in sterically constrained porphyrins [57].

The calix[4]arene-capped porphyrin (**91**) has been prepared in high yield by the reaction of calixarene with aldehyde followed by condensation with pyrrole [58]. The metallation of the new host with anhydrous ferrous chloride under nitrogen provides ferric porphyrin chloride, which is subsequently reduced to the corresponding Fe(II) complex (**92**). Exposure of (**92**) to oxygen in the presence of a coordinating base such as 1-triphenylmethylimidazole affords a dioxygen adduct that is stable for several hours at 20°C in chloroform. Compound (**92**) functions as an oxygen carrier.

5.2.4. Other porphyrin complexes

Electrochemical reduction of three iron(I) porphyrins in the presence of carbon monoxide has been investigated using cyclic voltammetry, thin-layer spectroelectrochemistry, UV-VIS and Raman spectroscopies [59]. Experiments have been carried out with the picket-fence porphyrin (**93**), and a basket-handle porphyrin and [Fe(III)(TFPP)Cl] (TFPP=*meso*-tetrakis(pentafluorophenyl)porphyrinato)

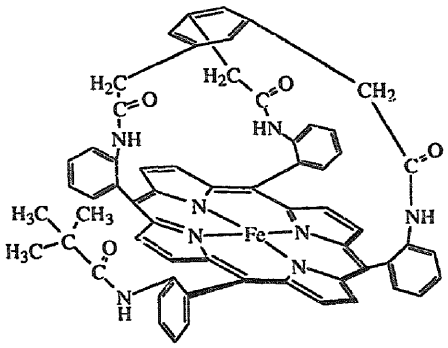

(89)

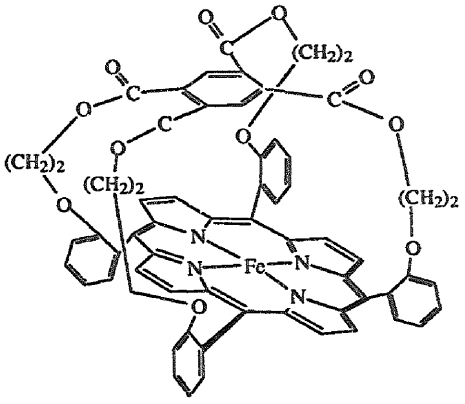

(90)

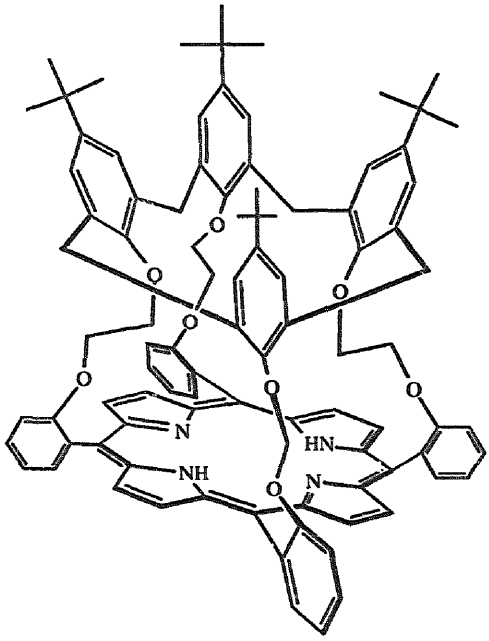

(91)

have been investigated for comparative purposes. In the absence of CO, the iron(I) porphyrins are reduced electrochemically to iron(0) complexes. When CO is present as an axial ligand, the formation of the phlorin anion complex (**94**) is favoured, which implies that in the carbonyl complexes the charge density is located on the

porphyrin ring rather than on the metal centre. Consequently, protonation of the *meso* carbons to produce iron(II) phlorin complex is observed. The presence of electron-withdrawing substituents such as fluorine atoms on the meso phenyl rings considerably slows down the protonation of the *meso* carbons.

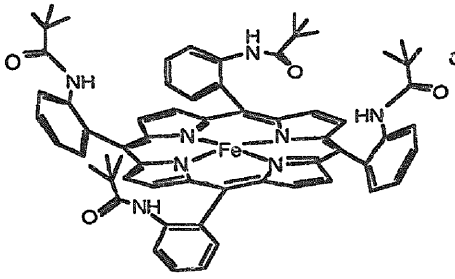

(93)

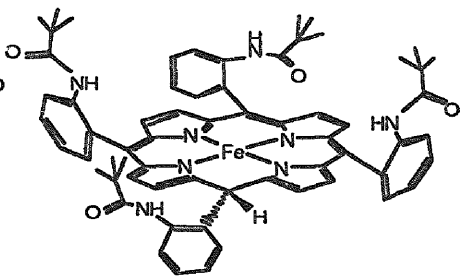

(94)

Ultraviolet-visible and resonance Raman (RR) spectroelectrochemical studies have been employed to investigate the process of one- and two-electron reductions of iron(III) *meso*-tetraphenyl- and *meso*-tetrakis(pentafluorophenyl)porphyrin in solvents of different coordinating abilities such as dimethylsulfoxide and butyronitrile [60]. Iron(I) complexes undergo photodecomposition which impedes spectral studies. When using a rotating cell, a RR spectrum is obtained which is similar to that of a low spin Fe(II) complex. In the absence of strong coordinating ligands the species derived from two-electron reduction of both porphyrins are better formulated as $[Fe(0)P]^{2-}$ complexes than $[Fe(I)P]^{\cdot}$ radical anions.

The [Fe(III)(TMP)-*N*-oxide] complex (**95**) has been obtained by reacting [Fe(III)(TMP)OH] with *meta*-chloroperoxybenzoic acid [61]. Raman Resonance spectra of this complex and its ^{18}O and ^{15}N derivatives have been measured. The results confirm a bridged structure of the Fe-O-N unity. The RR bands of the macrocycle such as C-C and C-N stretching modes are split into doublets due to lowering of symmetry and the 4 cm^{-1} downshift of C_m-phenyl stretching band suggests considerable distortion of the macrocycle.

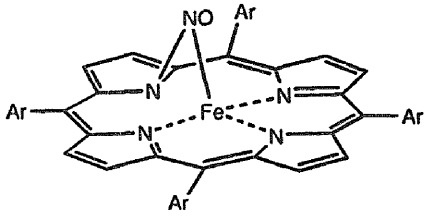

(95)

The visible and UV linear dichroism of *meso*-tetraphenylsulfonic porphyrin (**96**) (D_{4h} symmetry), protohemin III (C_{2v} symmetry) (**97**), and deuterohemin III (C_{2v} symmetry) (**98**) have been measured in stretched poly(vinyl alcohol) films in the

250-700 nm region [62]. For the metal-free *meso*-tetrakis(phenylsulfonic) porphyrin the absorption anisotropy is wavelength independent as for a circular absorber. Deutero- and protohemin III containing iron(III) centres exhibit wavelength-dependent dichroism indicating allowed transition moments of the linear type. It is concluded that the absorption of hemes should be considered as a simple combination of linear oscillators.

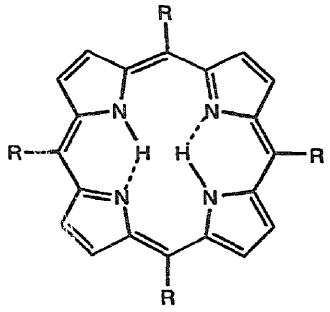

(**96**): R= -C_6H_4-*p*-SO_3H

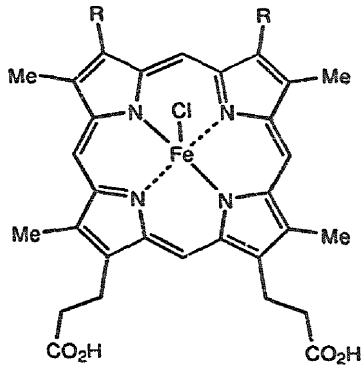

(**97**): R= -CH=CH_2; (**98**): R=H

A series of iron(III) porphyrins such as protoporphyrin IX dimethylester (**99**), mesoporphyrin IX dimethylester (**100**), deuteroporphyrin IX dimethylester (**101**) and octaethylporphyrin have been employed in the reaction of interconversion of some nucleic acid bases and nitric oxide in water-containing organic solvents under anaerobic conditions [63]. Cytosine and *N*-methylcytosine are converted to the corresponding uracils (35 and 40% of conversion), and adenine to hypoxanthine (12-15%). The nature of the porphyrin ligand does not appear to influence the conversion of cytosine to uracil. It is proposed that the reaction proceeds by the nucleic acid base attack upon a transient [(por)Fe(III)(NO)] adduct [(por)Fe(III)NO↔(por)Fe(II)NO^+] (por=(**99**)-(**101**), OEP). Water, as a nucleophile, competes with the nucleic acid base for the iron-complexed nitrosonium ion.

The diiron(III) porphyrins [XFe(III)TTPO-$(CH_2)_n$-OTTPFe(III)X] (X=Cl, Br, I), in which two tolylporphyrin units are linked via diether moieties (n=2 or 3) tethered at *ortho*-, *meta*- or *para*-positions of the *meso* phenyl moieties (**102**), have been synthesised [64]. Coordination of cyanide to these complexes has been investigated using ^1H NMR, ^2H NMR and IR spectroscopy. The high-spin monocyano complexes generated in the first step are converted into low-spin μ-cyano-bridged diiron(III) species with an intra- or intermolecular structure depending on the porphyrin geometry.

The preparation and structural determination of imidazolate-squeezed iron porphyrin dimers and a trimer linked by a rigid backbone molecule are described. 1,8-Anthracene (An) and *o*-phenylene (Ph) were chosen as linker molecules for Fe(III) tetraphenylporphyrin [65]. Two dimers, [(μ-Im)Fe_2{An(TPP)$_2$}(HIm)$_2$]Cl and [(μ-Im)$_2Fe_2${Ph(TPP)$_2$}(HIm)$_2$]Cl, and one trimer, [(μ-Im)$_2Fe_3${An$_2$

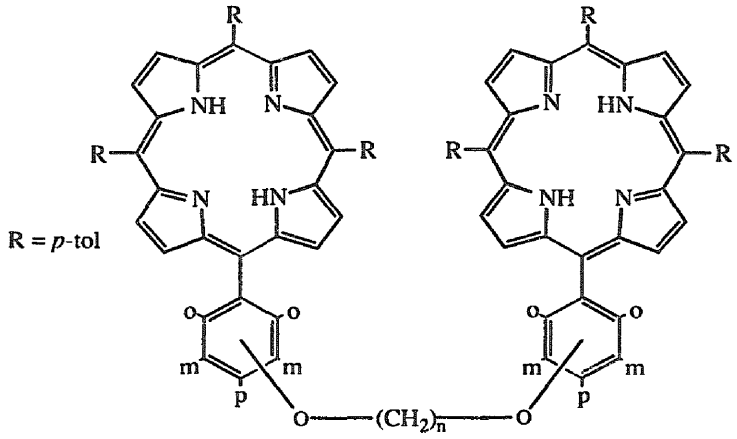

(102)

$(TPP)_3\}(HIm)_2]Cl$, have been obtained as crystals. The X-ray analysis of $[(\mu\text{-Im})Fe_2\{An(TPP)_2\}(HIm)_2]Cl$ reveals that the two Fe(III) ions are coordinated by an imidazolate molecule inside the molecular cavity. The N_{ax}-Fe bond distances are Fe-$N_{(Im)}$ = 1.95-1.96 Å and Fe-$N_{(HIm)}$ = 2.01-2.02 Å. These Fe-N_{ax} distances are compatible with a low-spin iron(III) state. The EPR and temperature-dependent magnetic susceptibility measurements show relatively large imidazolate-mediated antiferromagnetic exchange coupling ($-J = 15.3\text{-}29.4\ cm^{-1}$) between the Fe(III) ions of the dimers and the trimer.

A new paramagnetic ($S = 1/2$) (*p*-MeOTPP)Fe(III)$SnBu_3$ [*p*-MeOTPP = tetrakis(*p*-methoxyphenyl)porphyrinato] complex has been obtained by reacting the alkyliron(III) porphyrin with excess tributyltin hydride in toluene solution at ambient temperature [66]. Formation of the porphyrin tributyltin complex proceeds by a free-radical reaction initiated by homolysis of the alkyliron(III) C-Fe bond and generation of alkyl radicals followed by hydrogen abstraction from Bu_3SnH to yield the corresponding alkane and a Bu_3Sn radical. The latter subsequently adds to the Fe(II) porphyrin. The new complex is also generated by addition of Li tributyltin to the chloroiron(III) solution.

The water-soluble cationic porphyrin (**103**) has been synthesized via methylation of the corresponding *meso*-tetrakis(2,3,5,6-tetrafluoro-*N*,*N*-dimethyl-4-anilinyl) porphyrin and characterized by UV-VIS, NMR spectroscopies and electrochemistry [67].

Both faces of the porphyrin are protected by fluorine atoms which decrease both the extent of aggregation and the tendency for adsorbing at the surfaces. The iron porphyrin complex [Fe(**103**)] is monomeric in aqueous solution. Electrochemical studies carried out in water show that the iron(III)/(II) couple is *quasi*-reversible and pH-dependent with pKa for the iron(III) of 6.0 ($\mu = 0.1$ M).

Two new metalloporphyrins [Fe(TDCPN_6P)Cl] and [Fe(TFPN_4P)Cl] have been obtained in one step by nitration of *meso*-tetrakis(2,6-dichlorophenyl)- and *meso*-

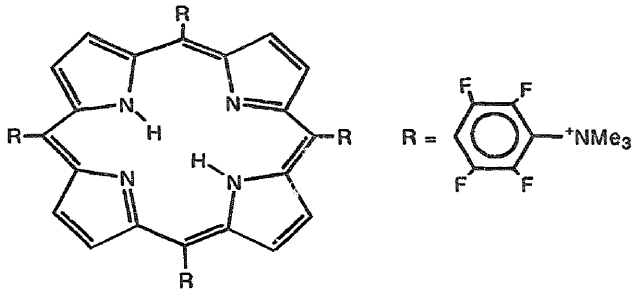

(103)

tetrakis(pentafluorophenyl)porphyrin with HNO_3 [68]. The former bears 4-6 nitro-substituents at the pyrrole β-positions whereas the latter accommodates up to four nitro groups. The complex [Fe(III)(TDCPN$_6$P)] is a very good catalyst for epoxidation of cyclooctene with diluted H_2O_2 in the absence of any co-catalyst. It is also a suitable catalyst for oxidation of such alkanes as cyclohexane and heptane by O_2 at 90°C under moderate O_2 pressure.

Iron(III)-porphyrin-based compounds serving as models for studying molybdenum-iron interactions in sulfite oxidase have been prepared by reacting 5-(3,4-dihydroxyphenyl)-10,15,20-tri-*p*-tolylporphyrin and 5-(2,3-dihydroxyphenyl)-10,15,20-tri-*p*-tolylporphyrin with $LMoO^{2+}$ (L=hydrotris(3,5-dimethyl-1-pyrazolyl)borate) followed by insertion of Fe(III) into the porphyrin ligand [69]. Two dimetallic complexes are obtained: FeCl(3,4-MoTPP) (**104**) and FeCl(2,3-MoTPP) (**105**) with Mo-Fe distances of 9.4 Å and 7.3 Å as determined from computer modelling studies. Upon addition of excess N-methylimidazole both complexes are transformed to the corresponding six-coordinate low spin Fe(III) complexes, each containing two imidazole axial ligands. The formation constants for these complexes are larger then those for related six-coordinate monometallic Fe(III) complexes of asymmetric porphyrin ligands. Cyclic voltammetry measurements indicate that the two metal centres in both [Fe(*N*-MeIm)$_2$(3,4-MoTPP)Cl] and [Fe(*N*-MeIm)$_2$(2,3-MoTPP)Cl] behave as independent one-electron couples. Simulation of the EPR spectra of these dimetallic complexes shows that weak anisotropic dipolar coupling dominates the interactions of the two metals in the former while weak exchange interactions predominate in the latter compound.

Iron complexes of a general formula [X$_2$(TPP)$_2$Fe$_2$(L)Cu$_2$Cl$_4$] (L=bis(acetylpyrazine)-ethylenediimine, X=Cl, N_3, imidazole, 1-methylimidazole, 2-methylimidazole, 4-methylimidazole and OMe) have been prepared [70]. Mössbauer, EPR spectroscopic and magnetic susceptibility measurements show that the spin state of the iron(III) centre depends on the nature of the axial ligand. For X=N_3, Cl, OCH_3, 1-MeIm and 2-MeIm, temperature independent high spin states ($S=5/2$) are found. Such axial groups as Im or 4-MeIm lead to temperature-dependent $^6A_1 \leftrightarrow {}^2T_2$ spin transitions. The magnetic properties of the investigated complexes imply weak antiferromagnetic interactions between Fe(III) and Cu(II) at low temperature.

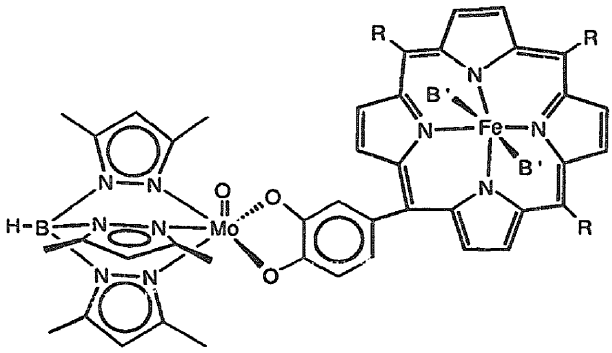

B' = *N*-MeIm, R = 4-MePh

(104)

The heterodinuclear complex $[(F_8TPP)Fe(III)\text{-}O\text{-}Cu(II)(TPA)]^+$ (**106**), where F_8TPP = tetrakis(2,6-difluorophenyl)porphyrinato and TPA = tris(2-pyridylmethyl)amine (**107**), has been isolated from a 1:1 mixture of $[(TPA)Cu(I)(CH_3CN)]^+$ and $[(F_8TPP)Fe(II)(pip)_2]$ (pip = piperidine) in O_2-saturated dichloromethane solution at -80°C followed by warming to 0°C [71]. Mössbauer studies indicate high-spin Fe(III) and moderately strong antiferromagnetic coupling between Fe(III) ($S_{Fe}=5/2$) and Cu(II) ($S=1/2$) ions. The X-ray measurements indicated linear μ-oxo-bridging ligand with unusual short metal-oxygen distances: Fe-O = 1.740(5) Å and Cu-O = 1.856(5) Å. The bridging oxygen atom is derived from dioxygen. The complex is a model for cytochrome *c* oxidase.

The reaction of [Fe(OEP)(py)(CN)] with an appropriate Cu(II) precursor produces a series of complexes $[(py)(OEP)Fe\text{-}CN\text{-}Cu(L/L')]^{2+/+}$ where $L/L' = Me_5dien/Me_2CO$ (**108**) and $bnpy_2/OTf$ (**109**), and L = TIM (**110**), cyclops (**111**) and cyclam (**112**) [72]. These molecules have been prepared and structurally characterised as a means of establishing the presence of a similar [Fe(III)-CN-Cu(II)] bridge unit in cyanide-inhibited cytochrome *c* oxidase and terminal quinol oxidases. In addition, the compounds $\{[(py)(OEP)Fe(CN)]_2Cu(cyclam)\}^{2+}$ (**113**), which has been shown to contain the [Fe(III)-CN-Cu(II)-NC-Fe(III)] bridge and $[(OEP)Fe\text{-}NC\text{-}Cu(Me_5dien)]^+$ (**114**) have also been prepared. Bent bridges have been found in compounds (**109**) (163°), (**110**) (147°) and (**111**) (159°) and the smallest angle has been observed in the doubly bridged complex (**113**) (140°, tetragonal octahedral). From infrared, magnetic and Mössbauer spectroscopic results, it may be concluded that cyanide-inhibited oxidised enzymes possess a tight [Fe(III)-CN-Cu(II)] bridge rather than a dinuclear site in which cyanide is bridged exclusively to one subsite, or interacts weakly with another subsite, or is hydrogen bonded at the uncoordinated end.

The reaction of $[Fe(OEP)(CN)(py)]$ with $[Cu(Me_6tren)(OH_2)(ClO_4)_2]$ results in the formation of $[(py)(OEP)\text{-}Fe\text{-}CN\text{-}Cu(Me_6tren)](ClO_4)_2$. The X-ray crystal

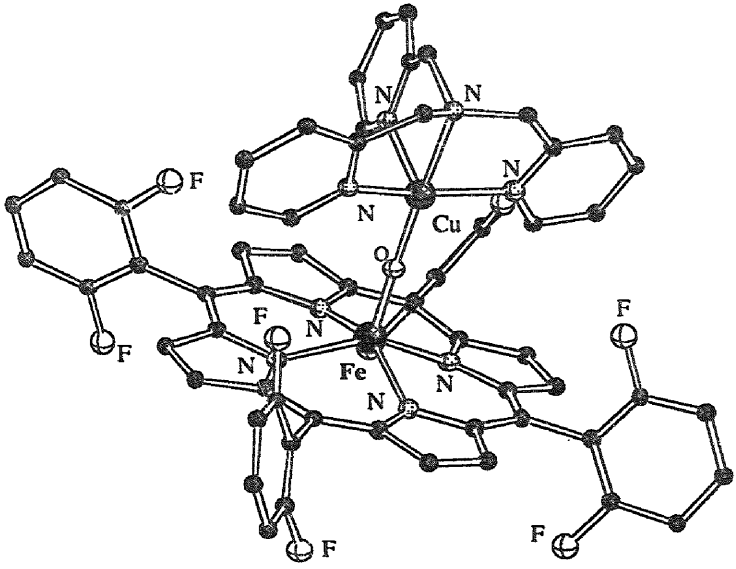

(106)

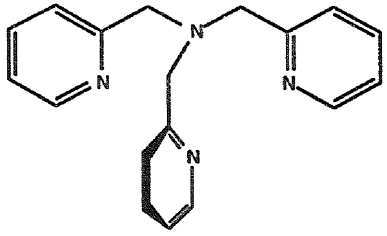

(107)

structures of the copper precursor and the cyanide-bridged species [(py)(OEP)-Fe-CN-Cu(Me_6tren)][SbF_6)$_2$ · Me_2CO have been reported [73]. The dinuclear assembly displays a virtually linear bridge unit Fe(III)-C-N-Cu(II), the structural refinement favouring a Fe-C-N-Cu over a Fe-N-C-Cu linkage. This observation was confirmed by the reaction of [Cu(Me_6tren)(CN)(ClO_4)$_2$] with [Fe(OEP)($OClO_3$)], from which the identical reaction product was obtained.

5.3. *Complexes with chlorins*

Preparation of oxoiron(IV) chlorin complexes [(**115**)Fe^{IV}=O(*N*-MeIm)] and [(**115**)Fe^{IV}=O], (*N*-MeI = *N*-methylimidazole), has been achieved by autoxidation of Fe^{II}(TPC) with dioxygen at -100 to -80°C. Reaction proceeds via formation of the μ-per-oxo-bridged iron(III) dimer followed by homolytic cleavage of the O-O

bond at -80°C. The six-coordinate imidazolate complex has been obtained by addition of *N*-methylimidazole to the μ-peroxo-bridged dimer at -80°C. Five- and six-coordinate oxoiron(IV) tetraphenylchlorin complexes have been characterized by UV-VIS, ^{1}H NMR and RR spectroscopies. Unusual splittings of the proton resonance into upfield and downfield region of the saturated pyrrole ring suggest deformation of the pyrrole ring of the chlorin complex. Oxoferryl chlorin complexes show Fe(IV)=O frequencies close to the corresponding porphyrin complexes. The investigated complex is the first model for a reaction intermediate in the catalytic cycle of cytochrome *d* [74].

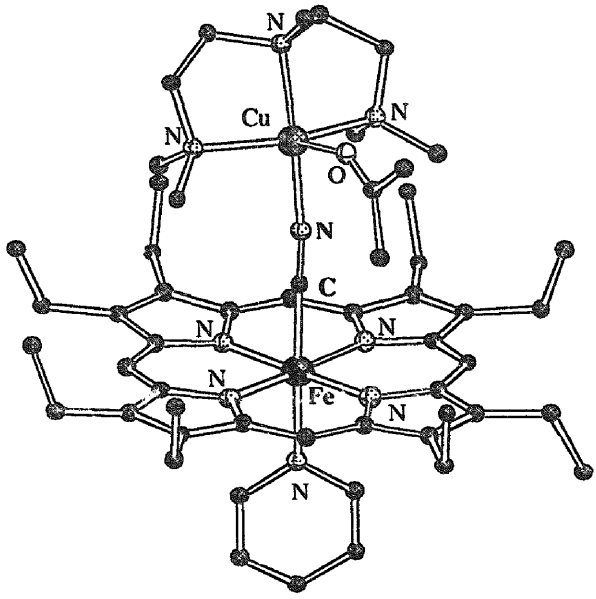

(108)

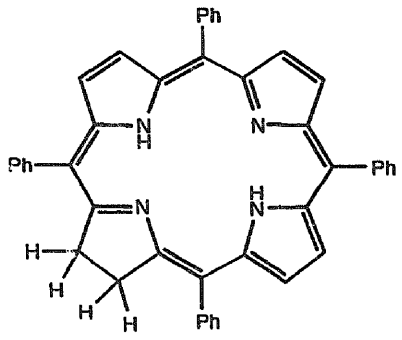

(115)

Peroxo-iron(III) chlorin complexes have been prepared by reacting chloro-iron(III)tetramesityl- (TMC) and octaethylchlorin (OEC) with superoxide in acetonitrile under argon [75]. The UV-VIS, EPR and IR spectra show similarities to those of the corresponding porphyrins, suggesting similar molecular and electronic structures. However, the paramagnetic deuterium NMR signals of the saturated pyrrole rings of the peroxo chlorin complexes exhibit an unusual large splitting into downfield and upfield regions, which is attributed to a large deformation of the saturated pyrroline rings in these complexes.

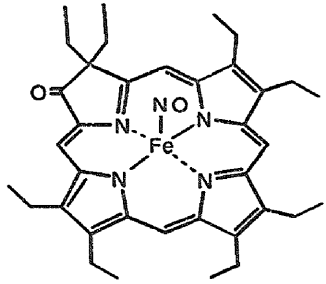

(116)

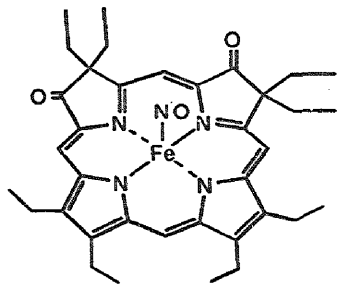

(117)

One-electron oxidation of nitrosyliron(II)oxoporphyrin complexes such as oxochlorin (**116**) and dioxoisobacteriochlorin (**117**) with silver hexafluoroantimonate in dichloromethane under argon affords the corresponding π-cation radicals with the bent geometry of the Fe-NO bond as shown by UV-VIS and IR spectroscopies [76].

The electronic structures and magnetic properties of some π-cation radical complexes of iron(III) and oxoiron(IV) chlorins have been examined [77]. The high and low spin iron(III) chlorin π-cation radicals exhibit well-resolved hyperfine-shifted NMR spectra, indicative of the a_2 radical state. Magnetic coupling between the iron spin and π-radical spin are revealed from the hyperfine shifts of the pyrroline ring protons. The oxoiron(IV) chlorin π-cation radicals for norbornene using two chlorins, tetramesitylchlorin (TMC) and tetrakis(2,6-dichlorophenyl)chlorin (TDCPC) are less reactive than the corresponding TMP porphyrin complex, this can not be attributed to the oxidation potentials of the chlorin macrocycles.

5.4. Miscellaneous tetrapyrrole complexes

The iron(III) corrole complex (**118**), containing an axial NO ligand has been synthesized and characterized by spectroelectrochemical methods [78]. The complex undergoes three one-electron oxidations and two one-electron reductions in benzonitrile and dichloromethane. The first two oxidations are reversible and afford Fe(III) cation radical and dication. Both maintain the NO ligand. Both reductions are also reversible and proceed without loss of the axial ligand. The first reduction is metal-centred and generates Fe(II) nitrosyl corroles.

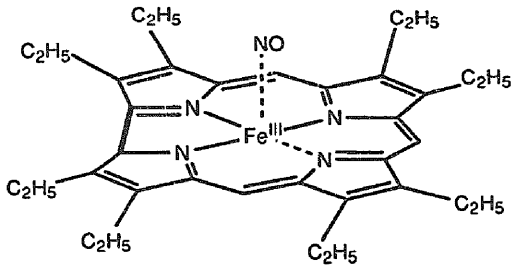

(118)

Electrochemical reduction and oxidation of iron(III) μ-oxo porphycene dimers [{(Pc)Fe}$_2$O], where Pc = the dianion of octaethylporphycene (**119**), etioporphycene (**120**), tetrapropylporphycene (**121**) or tetra-*tert*-butylporphycene (**122**), have been investigated and compared with the corresponding iron(III) μ-oxo-porphyrin dimers [79]. Electrochemical behaviour of porphycenes varies from that of porphyrins which are their structural isomers. The porphycene dimers undergo four reversible one-electron reductions and four reversible one-electron oxidations. The spectral data indicate that the site of the electroreduction during the first two one electron transfers is the conjugated π ring rather than Fe(III) centre. Such a behaviour is caused by the lower LUMO level of the μ-porphycene dimers when compared with the porphyrin complexes.

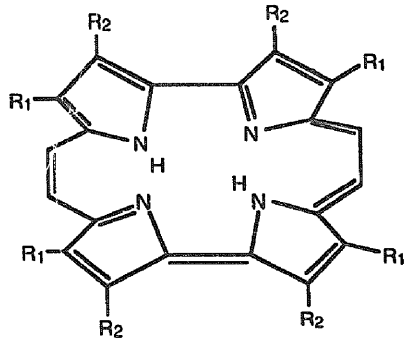

(**119**): R_1=R_2=Et; (**120**): R_1=Et, R_2=Me; (**121**): R_1=n-Pr, R_2=H;
(**122**): R_1=Bu^t, R_2=Et

Electrochemical and spectroelectrochemical measurements in dichloromethane and tetrahydrofuran have revealed that [Fe(III)(**123**)Cl] (**124**) undergoes reduction in three steps and oxidation in two one-electron steps [80]. The first reduction step is metal-centred while the remaining two reduction and two oxidation steps are ligand-centred. The corresponding μ-oxo-dimer [Fe(III)(**123**)]$_2$O undergoes four one-electron oxidations and four one-electron reductions and the resulting species is presumably [(Fe(**123**))$_2$)]$^{4-}$.

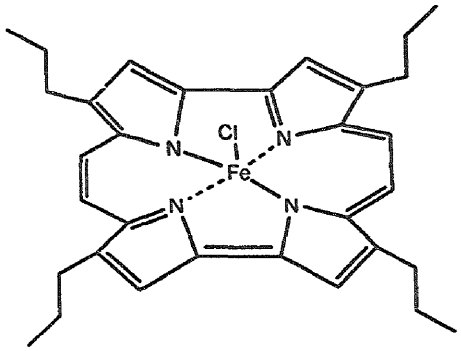

(124)

6. Complexes with oxygen donor ligands

6.1. Complexes with carboxylic acids and derivatives

The tetranuclear, mixed-valence ammonium inclusion complexes $[NH_4 \subset Fe_4L_6]$ (**125**, **126**) have been obtained by spontaneous self-assembly from the reaction of dialkylmalonates with methyllithium/iron(II) chloride and oxalylchloride at -78°C in thf, followed by workup with aqueous ammonium chloride. The complexes have been characterized by microanalytical data, FAB mass spectrometry, X-ray crystallography, Mössbauer spectroscopy (1 Fe(II), 3 Fe(III)), and electrochemistry [81].

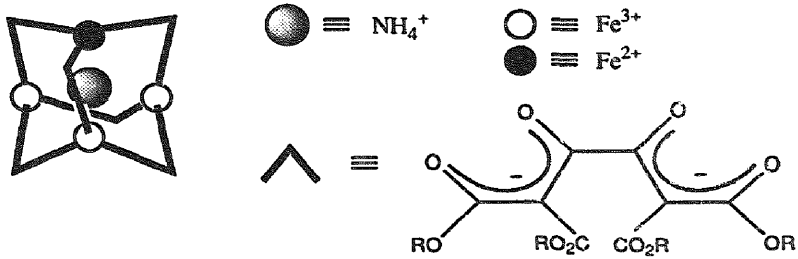

(**125**) R = Me; (**126**) R = Et

The equilibrium constants for the protonation of lactobionic acid (4-*O*-β-D-galactopyranosylgluconic acid) and its coordination with iron(II) have been studied by potentiometric methods in aqueous solutions. A comparative study between the behaviour of the iron(III)-lactobionic acid and iron(III)-D-gluconic acid systems has also been carried out. Coordination bonding sites and stereochemistry of metal-ligand interactions (**127**) were inferred from UV and NMR spectroscopies [82].

Iron citrate complexes have been postulated to be involved in the biological mobilization of iron and its extraction by plants from the rhizosphere. Two well-defined iron-citrate complexes $(Hpy)_2[Fe_2(\mathbf{128})_2(H_2O)_2] \cdot 2H_2O$ (**129**) and

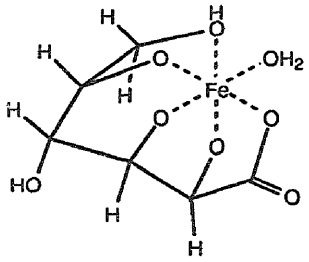

(127)

$(Hneo)_3[Fe_2(H\text{-}128)_3]\cdot nH_2O$ (130) (neo = neocuproine, (131)) have been synthesized and their solid state magnetic properties have been studied [83]. In complex (129) the two iron atoms are bridged by an alkoxide oxygen atom in two citrate groups while the two iron atoms in (130) are bridged by three citrate groups. Complex (129) shows antiferromagnetic exchange coupling between the iron atoms while the coupling in complex (130) is ferromagnetic, which is rare for face-shared d^5-d^5 systems.

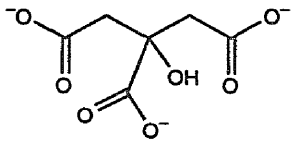

(128)

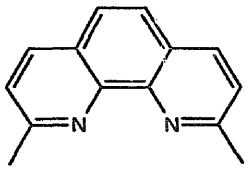

(131)

The phases $(X)Fe(II)Fe(III)(C_2O_4)_3$ ($X = NPr^n_4$, NBu^n_4, PPh_4) have been synthesised and characterized chemically, structurally and magnetically. They act as ferromagnets. The tetra-n-butyl ammonium salt shows unpredicted magnetic behaviour at low temperature–the magnetisation in field-cooled specimens becoming strongly negative [84].

The tris-chelated $[M(II)(bpy)_3]^{2+}$ cations, where $M(II)^{II}$ is a divalent transition metal, cause crystallization of anionic three-dimensional coordination polymers of oxalate-bridged metal complexes $[M_2(ox)_3]^{2n-}_n$. Two types of stoichiometric units of the anionic three-dimensional networks, with metals in different valence states, can be distinguished: $[M(II)_2(ox)_3]^{2-}$ and $[M(I)M(III)(ox)_3]^{2-}$. The Mössbauer spectra of the iron-containing compounds $[Fe(II)(bpy)_3][Fe(II)_2(ox)_3]$ (132) and $[Fe(II)(bpy)_3][Mn(II)_2(ox)_3]$ (133) and $[Fe(II)(bpy)_3][LiFe(III)(ox)_3]$ (134) are consistent with the stoichiometric formulae and the corresponding iron valence states. The magnetic susceptibility data for complexes (132), (133) and (134) in the temperature range 2 to 300 K are presented. Complexes (132) and (133) reveal antiferromagnetic ordering behaviour, indicated by negative Weiss constants, θ, of -28 and -33 K, respectively, whereas (134) exhibits the expected behaviour of single iron(III) ions [85].

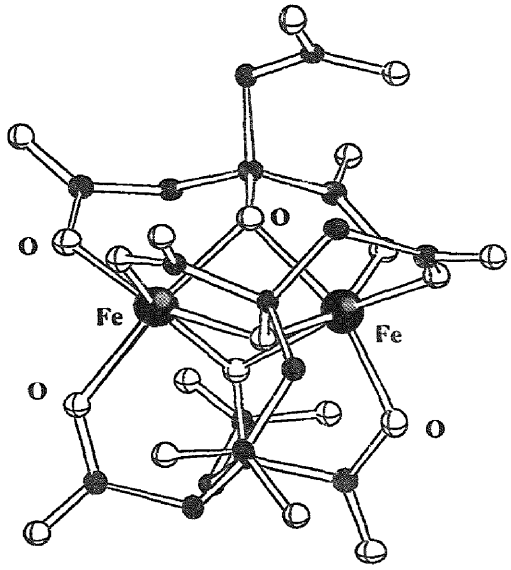

(130)

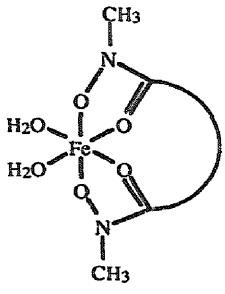

monomer, FeL^{+}

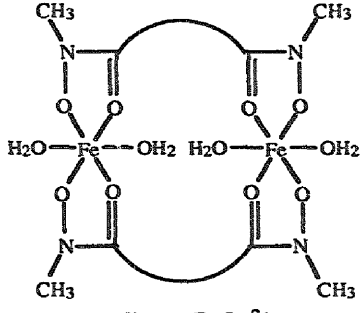

dimer, $Fe_2L_2^{2+}$

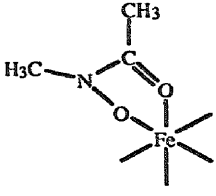

(137)

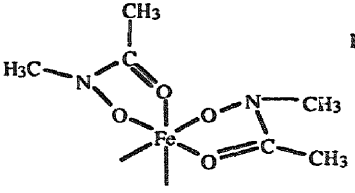

(138)

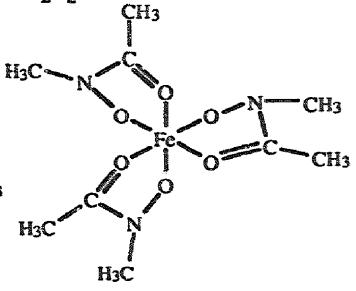

(139)

The stoichiometry of a series of 1:1 iron(III) complexes with model dihydroxamic acids $[CH_3N(OH)C(O)]_2(CH_2)_n$ (**135**), and with rhodotorulic acid (**136**), a natural dihydroxamate siderophore, have been studied by electrospray mass spectrometry (ESMS) [86–89]. The ESMS suggest that the model complexes exist in a dimeric form if $n=2$ or 4 and in a monomeric form if $n=8$ and for (**136**). When $n=6$ the complex is suggested to exist both in the monomeric and the dimeric form. Molecular mechanics studies show the same results. The dissociation of the [Fe^{III}(**135**)] complexes was also measured. The first step involves the dissociation of one hydroxamate group to give a mono(hydroxamato)iron(III) complex. For complexes with $n>6$ this step shows a first order dependence on pH, complexes with $n<6$ shows a second-order dependence on pH, and for $n=6$ two reactions are observed all in accordance with monomers for $n\geq 6$ and dimers for $n\leq 6$ suggested by the ESMS study. The dissociation rate constant for the dimeric complex depends on n, with $k_3=23$, 17, and 1.6 M^{-1} s^{-1} for $n=6$, 4, and 2, respectively. The rate-limiting dissociation constants for the monomeric complex are also dependent on n, with $k_6=0.13$ and 0.38 s^{-1} for $n=8$ and 7, respectively. The final step involving the removal of the last hydroxamate group was found to involve parallel acid-dependent and acid-independent pathways. The dissociation constants for this step does not vary significantly with n, but substitution of the methyl on the nitrogen for a proton increases the overall rate. Kinetic and equilibrium studies have also been made of the proton-initiated dissociation of the mono-, bis-, and tris-complexes of iron(III) with *N*-methylacetohydroxamic acid ((**137**), (**138**), (**139**)). The proton-dependent rate constants k_3, k_2, and k_1 for the dissociation of the tris-, bis- and mono-complexes are 8.6×10^3 M^{-1} s^{-1}, 1.02×10^2 M^{-1} s^{-1} and 3.2×10^{-3} M^{-1} s^{-1}, respectively. The corresponding equilibrium constants $\log K_3$, $\log K_2$ and $\log K_1$ are 1.06, -0.9, and -2.75 respectively. For the dissociation of the mono-complex there is also a proton independent dissociation pathway observed with the rate constant $k_1'=7.1\times10^{-3}$ s^{-1}. Proton NMR spectroscopy shows hindered rotation around the C-N bond.

6.2. *Complexes with other O donor ligands*

Bubbling dioxygen (1 atm, room temperature) through an acetonitrile solution of the nitrosyl dimer $[Fe(NO)_2Cl]_2$ in the presence of dppe leads to formation of the nitrato complex $[Fe(NO_3)_2Cl(O_2dppe)]$ (**140**). By analogy with $[Fe(NO_3)_2Cl(OPPh_3)_2]\cdot H_2O$, it is proposed that the metal is seven-coordinate in (**140**). Similar complexes containing the 1,2-bis(diphenylphosphino)ethene (dppen) ligand, *viz* $[Fe(NO_3)_2Cl(cis\text{-}O_2dppen)]\cdot H_2O$ (**141**) and $[Fe(NO_3)_2Cl(trans\text{-}O_2dppen)]\cdot H_2O$ (**142**), have been prepared [90]. The *cis*-dppen complex is proposed to have a structure corresponding to that of (**140**) while the *trans*-dppen complex may be a polymeric compound. Compound (**140**) may also be prepared by an oxygenation route in the presence of one equivalent of dppe. Oxygenation of $[\{Fe(NO)_2Cl\}_2(\mu\text{-dppe})]$ in the absence of phosphorus ligands results in the formation of $[Fe(NO_3)_2(O_2dppe)_2][FeCl_4]$ (**143**) while the corresponding dppen complexes (**144**) have been prepared by another route. Complexes (**141**) to (**144**) do not react with alkenes under anaerobic conditions but transfer oxygen to triphenylphosphine.

They also catalyse the aerobic oxidation of cyclohexene to mainly 2-cyclohexene-1-one and 2-cyclohexene-1-ol.

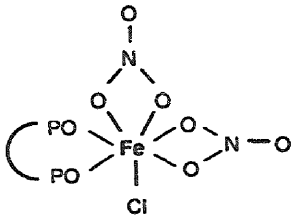

(140)-(142)

The complex $[Fe(MeLH)_6][NO_3]_3$ **(145)** (MeLH = 2-hydroxy-6-methylpyridine) has been formed by ligand transfer from $[Cu_6Na(MeL)_{12}][NO_3]$. The structure of **(145)** was determined by X-ray crystallography and revealed two independent formula units in the unit cell [91]. The iron atoms are octahedrally coordinated with only small distortions. The protons on the pyridine nitrogens are hydrogen bonded to the oxygen atoms of the nitrate anions. One of the units has three nitrogen atoms involved in hydrogen bonding while all six nitrogen atoms are involved in hydrogen bonding in the other unit.

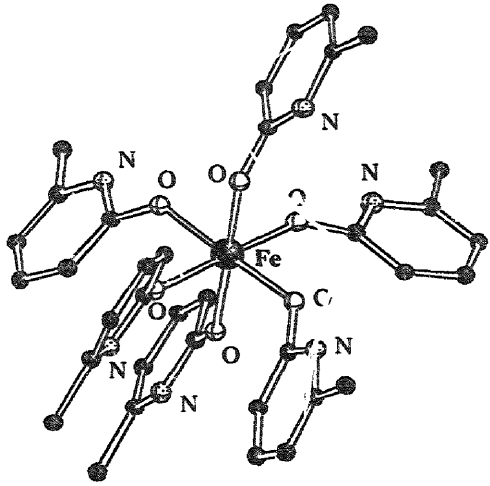

(145)

Four octadentate derivatives of terephthalamide desferrioxamine B **(146)**, derivatives **(147)** to **(150)**, have been studied as ferric ion complexing agents by potentiometric, spectrophotometric, and NMR spectroscopic titrations [92]. All four form six-coordinate 1:1 ferric complexes in aqueous solution. For the catecholate derivatives **(147)** to **(149)**, the tris-hydroxamate ferric complex forms at low pH. As the pH increases, the terminal hydroxamate group is replaced by a catecholate group.

The inverse is true for (**150**), where the hydroxamate is replaced by the more acidic hydroxypyridinonate as the pH decreases. Stability constants obtained represent the first example of formation constants for bis-hydroxamate monocatecholate ferric complexes.

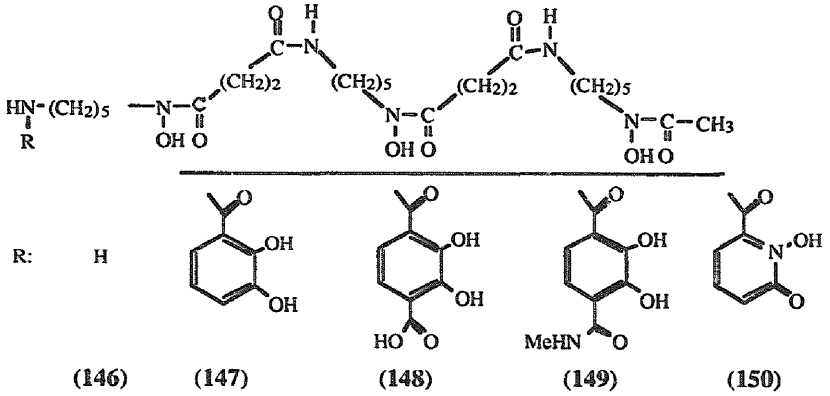

(**146**) (**147**) (**148**) (**149**) (**150**)

In an attempt to mimic enterobactin, an acyclic siderophore, a pre-assembled iron complex (**151**) was crosslinked with PEI (poly(ethylene imine)) [93]. The formation of amide linkages in the complex was detected with IR-spectroscopy but it was not possible to see whether the resultant complex (**152**) was bicapped. The chelation stability for (**152**) was measured using CDTA. The complex showed greater stability in acidic pH and pM values greater than those of several other analogues.

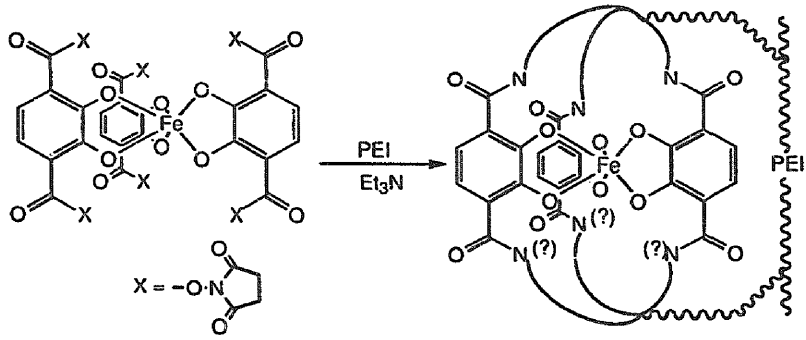

(**151**) (**152**)

The coordination chemistry of the macrobicyclic tris-catecholate ligands (**153**)-(**156**) with Fe^{3+}, V^{4+}, Ti^{4+}, and Ga^{3+} has been investigated in order to model the coordination behaviour of the tris(catechol)-siderophore enterobactin. The UV-VIS spectra of the Fe(III) complexes indicate that they have pseudo-octahedral coordination geometry around the central atom [94].

Catecholato-iron complexes were isolated from the reaction of $FeCl_3$ with (**157**),

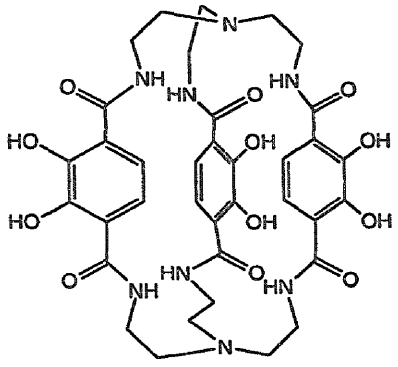

(153)

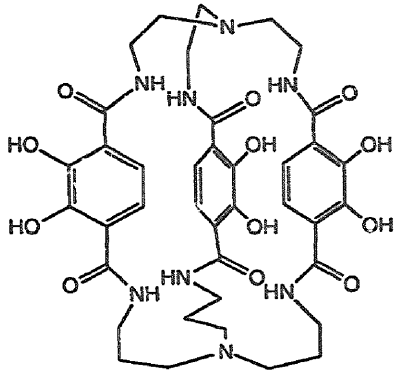

(154)

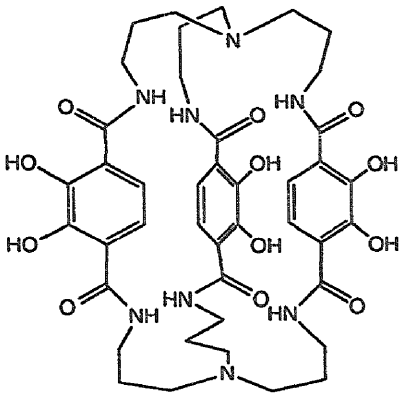

(155)

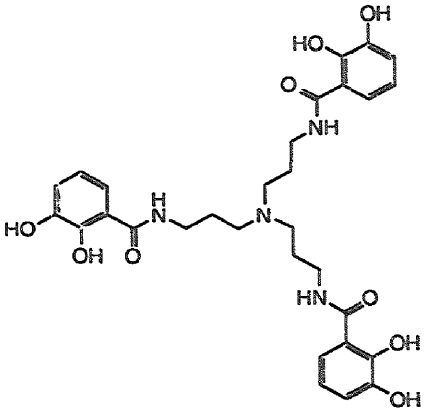

(156)

(158) or (159) in thf in the presence of pyridine [95]. The complexes of 1 and 2 are dimeric in the solid state but monomeric in solution (thf). These monomeric complexes are formulated as [FeCl(157)(py)$_2$] and [FeCl(158)(py)]$^+$H$^+$, respectively. The complex containing (159) is a monomeric six-coordinate complex [FeCl(159)(py)$_2$]$^+$H$^+$ both in the solid state and in thf. Reactivity of the isolated catecholatoiron complexes with O_2 reveals that a stable chelated catecholate species may be activated to be reactive with O_2 in the catalytic oxygenation of catechols. It has been found that the catecholato-iron complexes becomes reactive with oxygen in the presence of an excess of catechols. Spectroscopic studies indicate that catecholate ligand exchange plays an important role in the activation of the catecholate ligand.

Reaction of 4-*tert*-butylpyridine (Bupy) with [Fe(160)$_3$] [(160)=3,6-di-*tert*-

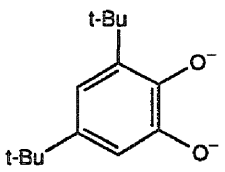

(157)

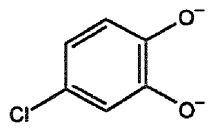

(158)

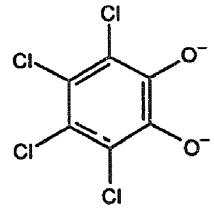

(159)

butylbenzoquinone] leads to the formation of $[Fe(Bupy)_2(\mathbf{160})_2]$ (**161**) [96]. Electrochemical and spectroscopic measurements indicate that the metal is high-spin Fe(III) and that (**160**) exists in both its catecholate and semiquinone form in (**161**). Cyclic voltammetry of (**161**) reveals two redox couples at -0.34 and -0.86 V for the quinone ligands and an Fe(III)/Fe(II) couple at -1.42 V. Structural characterization of (**161**) by X-ray crystallography showed that the molecule is in its *trans* isomeric form and that crystallographically imposed inversion symmetry disorders the catecholate and semiquinone ligands. A low-energy transition at 2100 nm is tentatively assigned as a catecholate→Fe(III) CT band. Unlike its Mn and Co analogues, (**161**) does not show evidence for a valence tautomeric equilibrium.

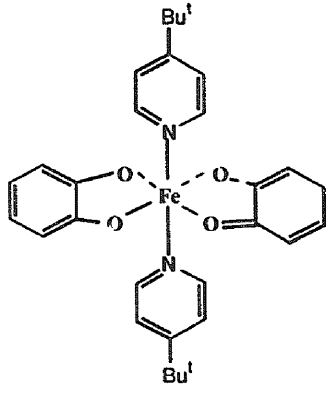

(161)

Complex formation between iron(II) and 2-hydroxy-1,4-naphthoquinone including both protonated, anionic and reduced forms of the ligand have been electrochemically and spectroscopically investigated in dmso [97]. The protonated and anionic ligands did not give any stable complexes. The iron complex with the reduced form of the ligand has a 1:2 stoichiometry and a formation constant of 3.5×10^{25}. Magnetic susceptibility measurements reveal an intramolecular charge-transfer between the iron and one of the radical ligands giving an iron(III) character to the metal ion.

7. Complexes with sulfur donor ligands

The compounds [Fe(**162**){$N(SiMe_3)_2$}] (**163**) and [Fe(**162**)$_2$] (**164**) were synthesized by the reaction of one or two equivalents of the new thiol (**162**) with [Fe{$N(SiMe_3)_2$}$_2$] [98]. The structural and spectroscopic data support the view that the iron centres in (**163**) and (**164**) are primarily two-coordinate with minor interaction with π-electron density of the *ortho*-mesityl group of the thiolato ligand.

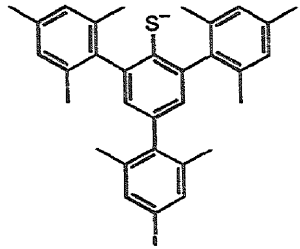

(**162**)

Analysis of the vibrational spectra for a series of iron(III) tetrathiolate complexes, including $[Fe(SMe)_4]^-$, $[Fe(SEt)_4]^-$, and $[Fe(S_2$-*o*-xyl$)_2]^-$ has permitted the reanalysis and modelling of previously published RR spectra of oxidised rubredoxin in which Fe^{3+} is bound to four cysteinate side chains [99]. The spectra of the rubredoxin analogues reveal (i) lowering of symmetry from T_d, due to the S-C bonds being oriented out of the S-Fe-S planes (ii) splitting in the case of $[Fe(SMe)_4]^-$ due to inequivalence of the S-Fe-S angles (iii) elevation of the υ_1 Fe-S breathing frequency and (iv) mixing of Fe-S stretching and S-C-C bending modes due to the chelate ring constraints in $[Fe(S_2$-*o*-xyl$)_2]^-$. The rubredoxin reveals a dominant influence of Fe-S/S-C-C mixing due to 180° FeS-C-C dihedral angles for two of the cysteinate ligands.

The complexes [Fe(L)(**165**)] [complex (**166**) with L=PMe_3; (**167**), PMe_2Ph, (**168**), PBu_3; (**169**), $PMePh_2$; (**170**), N_3] and [Fe(**165**)]·thf (**171**) have been prepared [100]. The phosphine complexes contain low-spin Fe(II) centres and chiral [Fe(**165**)] cores while (**170**) is an Fe(II) high-spin complex with an achiral [Fe(**165**)] core. The phosphine ligands in complexes (**166**)-(**170**) are labile and may be substituted by CO but not by N_2. Repeated attempts to transform the azido ligand in (**170**) into N_2 by thermal or oxidative means failed. Complex (**171**) contains a five-coordinate Fe centre. The structure and distances of (**171**) resemble the [Fe(**165**)] cores of low-spin [Fe(L)(**165**)] complexes, whereas the paramagnetism and high reactivity of (**171**) are typical of high-spin [Fe(L)(**165**)] complexes. The new complexes [Fe(L)("N_RS_4")] [R=Me (**172**), L=PMe_3 (**173**), N_2H_4 (**174**), NO^+ (**175**), NO (**176**); R=CH_2CH_2COOMe, L=PMe_3 (**177**), N_2H_4 (**178**)] have been synthesized [101]. A 19-electron low-spin complex is prepared by reduction of (**175**) with tetraethylammonium azide.

8. Complexes with phosphorus donor ligands

The complexes *trans*-$[Fe(L\text{-}L)_2I_2]BF_4$ where L-L = *o*-$C_6H_4(PMe_2)_2$, *o*-$C_6H_4(AsMe_2)_2$ or *o*-$C_6F_4(PMe_2)_2$, have been isolated and structurally characterized [102]. The UV-VIS spectra of the iron(III) iodo complexes strongly resemble those of *trans*-$[M(L\text{-}L)_2I_2]^+$ (M = Ru, Os) and suggest that the complexes are pseudo-octahedral iron(III) iodine complexes with *trans* 6-coordinate structures (D_{2h}).

9. Complexes with mixed-donor ligands

9.1. Complexes with mixed N,O-donor sets

The dinuclear complex $[Fe_2(\mathbf{179})(imidazole)_2(CH_3OH)_2](ClO_4)_2 \cdot 2CH_3OH$ (**180**) has been prepared by reacting the tetraaminodiphenol macrocyclic ligand (**179**) with $Fe(ClO_4)_2.6H_2O$ and spectroscopically characterized. Cyclic voltammetric study of (**180**) shows a irreversible oxidation at 1.02 V *vs* SCE. Variable-temperature magnetic measurements indicate that (**180**) exhibits antiferromagnetic exchange coupling with $J = -6.3\ cm^{-1}$.

The effect on the structure of [Fe(II)(5-NO_2-sal-N(1,4,7,10))] (**181**) upon a two-step spin-state conversion has been studied [103]. The X-ray crystal structures have been determined at 292, 153 and 103 K. Complex (**181**) is linked into infinite chains in the solid state through two sets of N-H···O(nitro) hydrogen bonds. Two spin-state conversions ($S = 2 \leftrightarrow S = 0$), each involving approximately 50% of the molecules, occur in the same temperature range. Two equally distributed sets of molecules in the material could therefore be distinguished. The two spin-state conversions were only associated with moderate changes in M-L distance and L-M-L angles. The two steps also showed signs of cooperative effects; magnetic susceptibility and Mössbauer studies showed that the second step was steeper than the first and DSC experiments showed that the heat capacity peak corresponding to step two is sharper than that corresponding to step one.

A lipophilic iron(III)complex of the new hexadentate ligand (**182**) has been reported [104]. The complex has been characterized by IR, NMR and UV-spectroscopy and the X-ray structure of [Fe(**182**)] (**183**) has been determined. In the structure two of the pendant phenolate moieties have a propeller-like conformation while the third does not; however, the ^{1}H-NMR spectrum of (**183**) shows that the three pendants are equivalent, suggesting that the structure is semi-rigid.

Two iron(III) complexes with the dinucleating ligands (**184**) and (**185**), *viz.* $[Fe_2(\mathbf{184})(O_2P(OPh)_2)_2]BPh_4 \cdot CHCl_3 \cdot CH_3OH$ (**186**) and $[Fe_2(\mathbf{185})(O_2P(OPh)_2)_2]ClO_4 \cdot H_2O$ (**187**), have been prepared as models for the active site of purple acid phosphatase [105]. The synthesis and crystal structures of the iron(III) complexes with these ligands are reported. The electronic spectra of (**186**) and (**187**) reveal relatively intense $\pi \rightarrow \pi^*$ charge-transfer bands from the phenolate oxygens to the

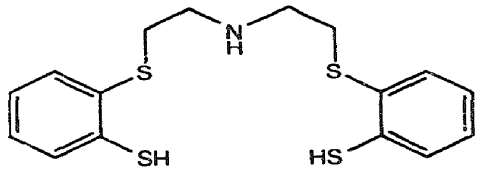

(165)

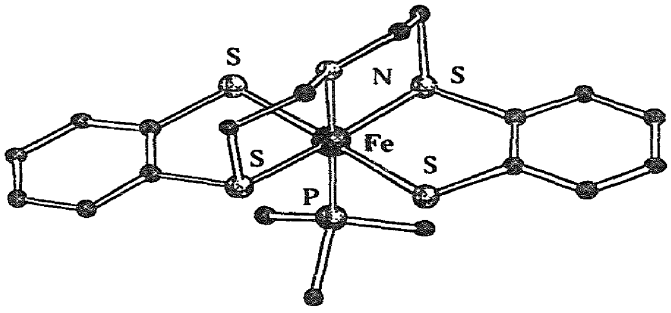

(166)

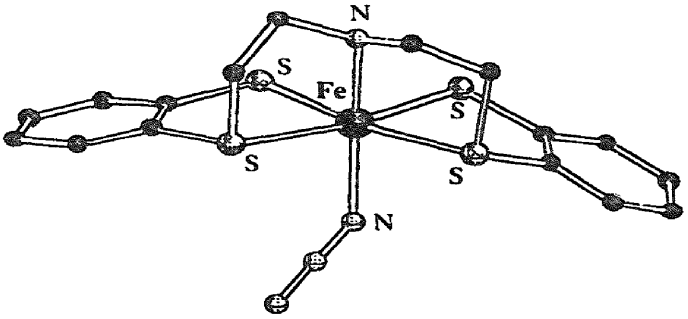

(170)

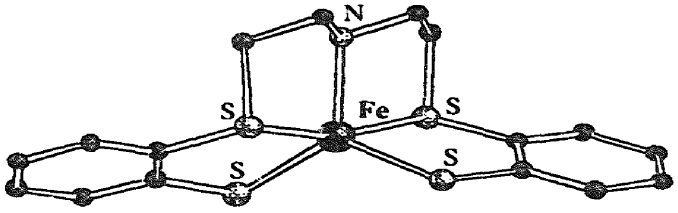

[Fe(165)] core of (171)

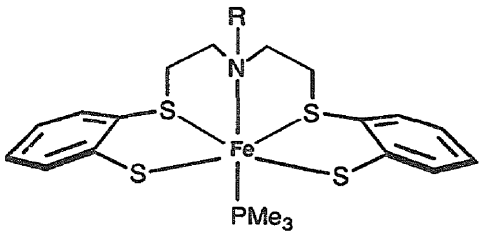

(177)

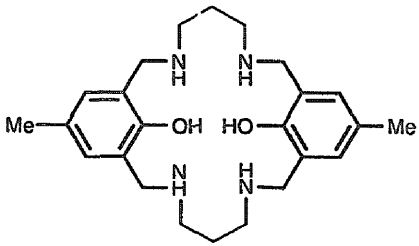

(179)

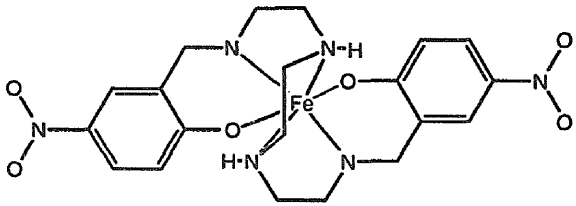

(181)

Fe(III) ions. The Mössbauer spectra of both compounds indicate that the metals are high spin Fe(III).

Complex (**188**) is the first structurally characterized model complex of a PAP enzyme that reproduces the unsymmetrical coordination of a terminal phenolato ligand to a diiron centre [143]. Solid-state magnetic studies have shown that the electronic structure of complex (**188**) is similar to that of the active site of the enzyme. Electrochemical studies demonstrate that (**188**), like the PAP enzymes, has stable Fe(III)Fe(III) and Fe(II)Fe(III) forms, and that the terminal phenolato ligand destabilizes the diiron(II) state, both in terms of electrochemical potentials and of chemical reactivity.

Iron(III) complexes of the type $(L)Fe_2(O_2CR)_3$ (L=(**189-192**), R= $-C_6H_5$, $-CH_2CH_3$, $-CH_3$) have been prepared [107]. They were characterized by

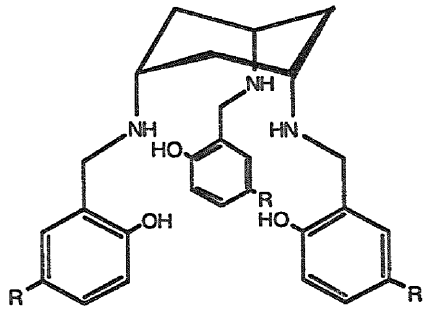

R = NO$_2$

(182)

Mössbauer, IR, UV-visible and ^{1}H-NMR spectroscopy as well as cyclic voltammetry. Varying of the carboxylate ligands did not alter the electronic nature of the complex but additional alkyl substituents on the macroligand stabilized the iron(III) centres.

The iminoquinone complex [Fe(**193**)$_2$Cl$_2$](FeCl$_4$) has been prepared [108]. Reduction converts the ligand to its semiquinone form and the structure of the resultant complex Fe(**193**-SQ)$_2$Cl (**194**) has been determined by X-ray crystallography. The complex possesses a trigonal bipyramidal structure with the chloro ligand in an equatorial site. Cyclic voltammetry show two oxidations and two reductions in the range $\pm$1.2 V (*vs* NHE) occurring at the ligand and one further reduction at the metal at -1.427 V.

The rapid auto-oxidation of O_2 with [Fe(II)(DPAH)$_2$] (DPAH$_2$=2,6-dicarboxypyridine) has been investigated [109]. The reaction yields HOOH and [Fe(III)(DPAH)(DPA)] ((**195**); $k_1 = 1.8 \pm 0.5\ M^{-1}\ s^{-1}$). The hydroperoxide reacts further with excess [Fe(II)(DPAH)$_2$] and to yield the Fenton reagent, [(DPAH)$_2$Fe(II)OOH] (**196**)+pyH$^+$. The further reaction of the Fenton reagent (**196**) with excess Fe^{II}(DPAH)$_2$ gives (**195**). Reaction of (**196**) with excess cyclohexane and PhSeSePh results in the formation of cyclo-C_6H_{11}SePh with a kinetic isotope effect (k_{C6H12}/k_{C6D12})=2.2. Reaction of (**196**) with excess O_2 leads to the formation of the adduct (**196**)·O_2, which reacts with excess cyclohexane to form cyclohexanone.

Molecular mechanics studies of ferric chelates of low molecular weight have been carried out in order to obtain the AMBER all-atom force field parameters for transferrin. The crystal structures of the Fe(III) complexes of (**197**), TACN-1,4,7-triacetic acid (TCTA), and (**198**) were fitted [110]. Conformational energies and energy minimized molecular structures of (*R,R*), (*R,S*), and (*S,S*) isomers of (**197**) were calculated both *in vacuo* and in aqueous solution using a generalized Born/surface area (GB/SA) continuum treatment. The rms deviations between geometries calculated with the GB/SA treatment and geometries from published crystal structures were calculated for the Fe(III)(**197**), Fe(III)TCTA, Fe(III)(**198**), and Fe(III)(**199**). The Fe(III)(**197**) complex shows an increasing stability according to (*S,S*)<(*R,S*)<(*R,R*); the order is the same for *in vacuo* and

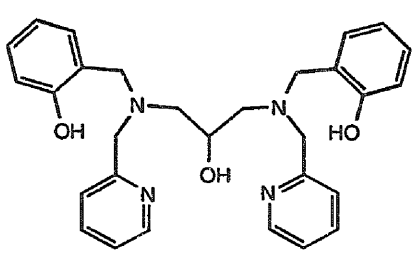

H_3-(184)

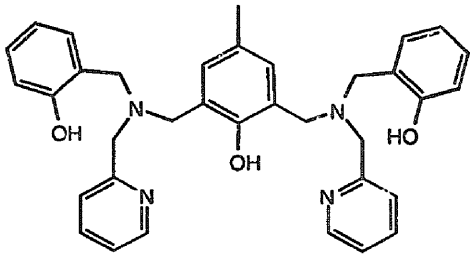

H_3-(185)

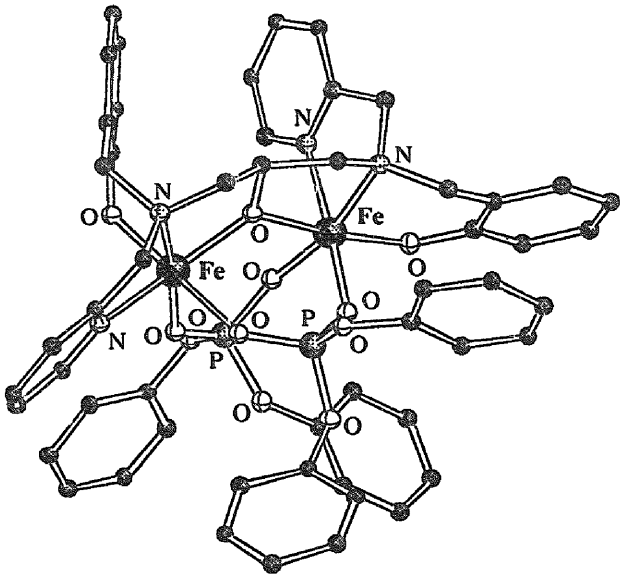

(186)

aqueous solution calculations but the energy differences are smaller in aqueous solution. The calculated order of stability for three different conformers of Fe^{III}(**199**) were *trans*-(O_6) < *trans*-(O_5,O_6) < *trans*-(O_5). The MM calculations predict that an equatorial coordination plane containing chelate rings in a 6,5,6 combination of sizes with two 5-membered axial rings would give the optimum stability.

The kinetics of the reaction of dioxygen with the well-characterised compounds [Fe_2(**200**)(OBz)](BPh_4)$_2$ (**201**), [Fe_2(**202**)(OBz)](BPh_4)$_2$ (**203**), and [Fe_2(**204**)(OBz)](BF_4)$_2$ (**205**) have been studied [111]. Compounds (**203**) and (**205**) follow a second-order rate law, whereas compound (**201**) displays a partial order of 0.65 with respect to dioxygen which may imply a different reaction mechanism. An Eyring analysis of the kinetic data showed compounds (**203**) and (**205**) to have activation enthalpies indicative of a simple addition mechanism. The parameters for

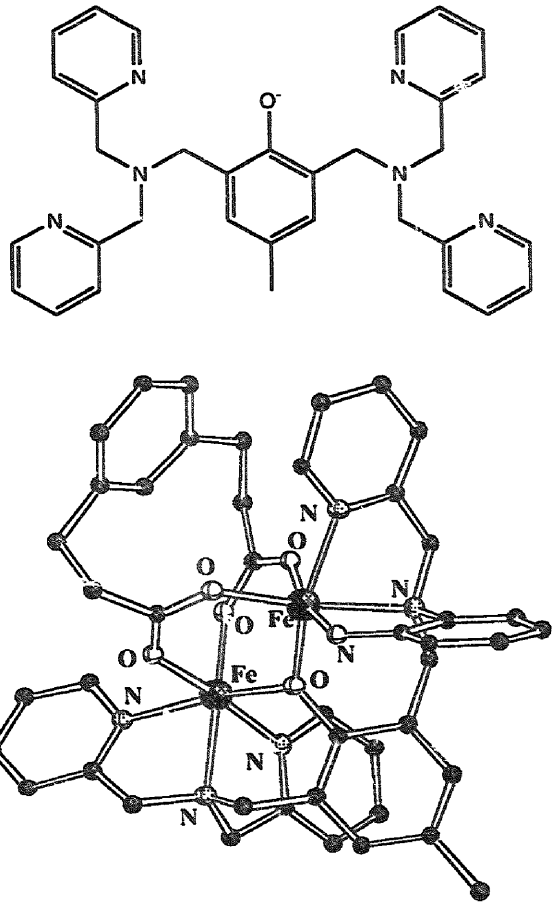

(188)

compound (201) differ substantially from the others. Although compound (201) has a vacant coordination site for dioxygen binding, it is sterically impeded and a structural rearrangement is required before inner-sphere coordination of O_2 is possible; this may explain the higher activation barrier.

The ground state electronic structure of $[Fe_2(206)_2]^{2-}$ has been studied by EPR and Mössbauer spectroscopy [112]. Mössbauer spectroscopy indicates that there are two equivalent ferrous sites. The anion $[Fe_2(206)_2]^{2-}$ bears some similarities to the diferrous clusters of proteins; the exchange coupling is ferromagnetic like that observed in the hydroxolase component of methane monooxygenase and the azide adducts of ribonucleotide reductase B2 and deoxy-hemerythrin.

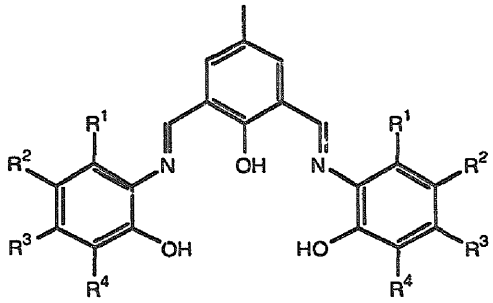

(189): $R^1=R^2=R^3=R^4=H$; (190): $R^2=CH_3$, $R^1=R^3=R^4=H$
(191): $R^3=CH_3$, $R^1=R^2=R^4=H$; (192): $R^2=R^4=CH_3$, $R^1=R^3=H$

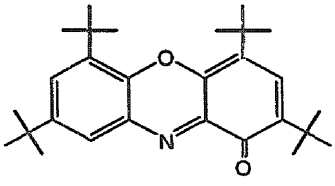

(193)

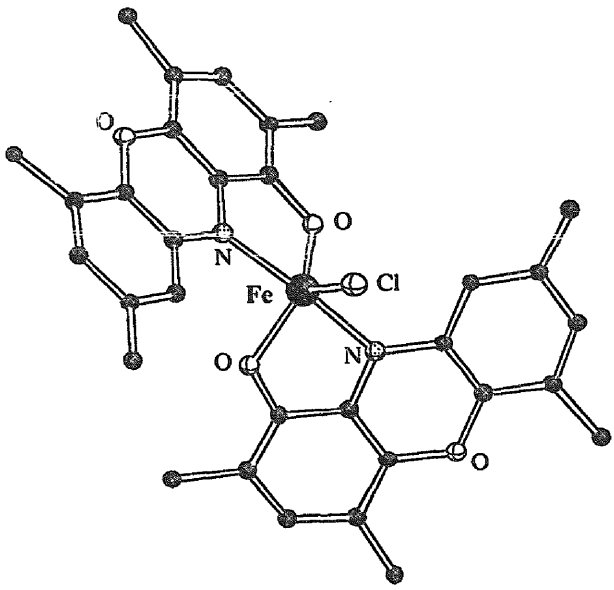

Methyl carbon atoms of ^{t}Bu groups omitted for clarity

(194)

9.2. *Complexes with mixed N,S-donor sets*

The effects of a change of temperature and pressure on the spin-state transition in $[Fe(207)_2(NCS)_2]$ have been studied [113]. At atmospheric pressure the compound has a spin-transition around 175 K with a hysteresis width of 7.1 K. The application of pressures in the range 0.001-1.90 kbar gave no changes in the transition temperatures but the hysteresis width decreased significantly to a $\Delta T_c = 5.7$ K at

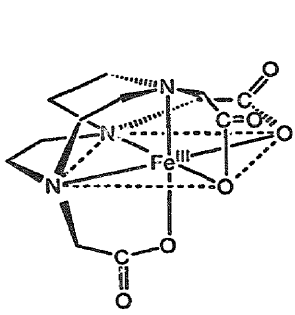

Fe(III)(197)

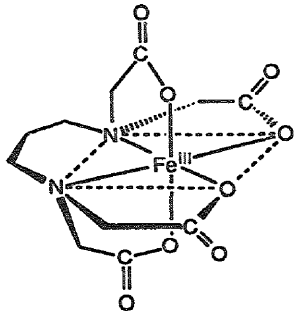

Fe(III)(198)

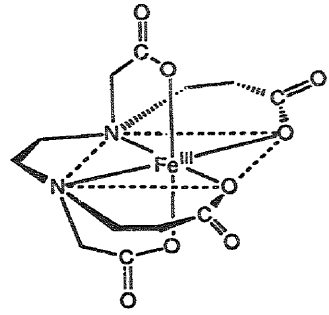

Fe(.II)(199)

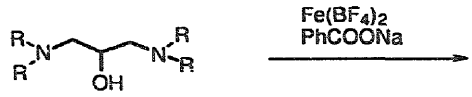

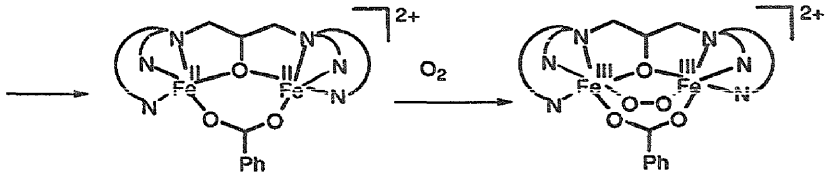

R =

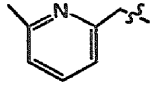

(200)

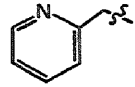

(202)

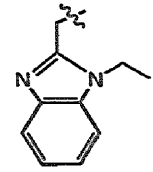

(204)

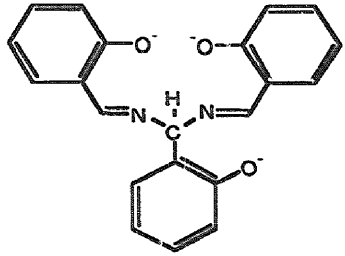

(206)

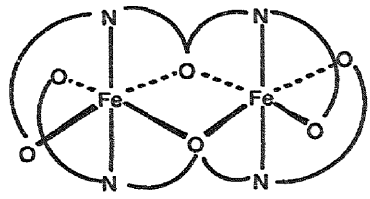

$Fe_2(206)]^{0,1-,2-}$

1.90 kbar. The decrease of $(\Delta T_c)^{1/2}$ was found to be linear with pressure within the accuracy of the measurement.

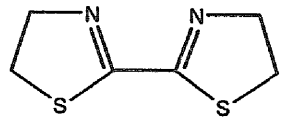

(207)

9.3. *Complexes with other mixed-donor ligands*

A series of stable high spin Fe(III) complexes of ligands (**208**)-(**210**), containing $S_2N_2O_2$ ligand donor sets, which display relatively low Fe(III)-Fe(II) reduction potentials have been prepared from the reaction of hexadentate triazene 1-oxide thioethers with iron(III) nitrate followed by addition of sodium perchlorate [114]. The compound $[Fe(Me_3L)]ClO_4$ may represent the first example of a structurally characterised high-spin trivalent iron ligated with thioethers.

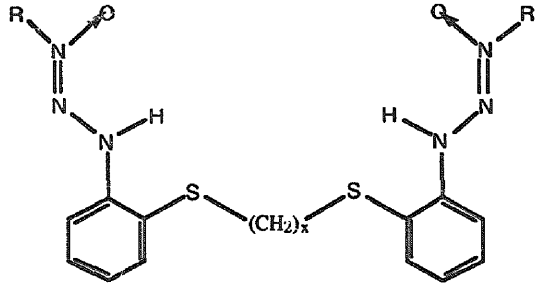

(**208**): R = Me, x = 2, (**209**): R = Ph, x = 2, (**210**): R = Me, x = 3

10. Iron-oxo clusters

10.1. *Di- and trinuclear iron-oxo and hydroxo-clusters*

The reaction of $Fe(ClO_4)_3 \cdot 10H_2O$ with $TPA \cdot 3HClO_4$ [TPA=(**212**)] and four equivalents of triethylamine affords the dinuclear complex $[Fe_2O(TPA)_2(H_2O)(ClO_4)](ClO_4)_3$ (**213**) [115]. The crystal structure of (**213**) clearly shows a nearly linear (μ-oxo)diiron (III) core, with an Fe-O-Fe angle of 174.1° and a Fe-Fe distance of 3.57 Å. Treatment of (**213**) with one equivalent of triethylamine affords $[Fe_2O(H_3O_2)(TPA)_2](ClO_4)_3$ (**214**). Compound (**213**) is stable in acetonitrile while compound (**214**) converts to $[Fe_2O(TPA)_2(CH_3CONH)](ClO_4)$ (**215**). Compound (**215**) can be prepared independently by treatment of (**214**) with

acetamide. The conversion of (214) to (215) displays *pseudo* first-order kinetics. Addition of water to the reaction slows the reaction rate, suggesting that water and acetonitrile compete for binding to the iron. Once coordinated, the acetonitrile may be attacked by the hydroxide on the other iron resulting in the formation of the bridging acetamidato ligand.

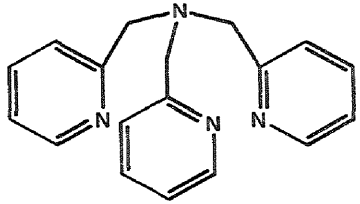

(212)

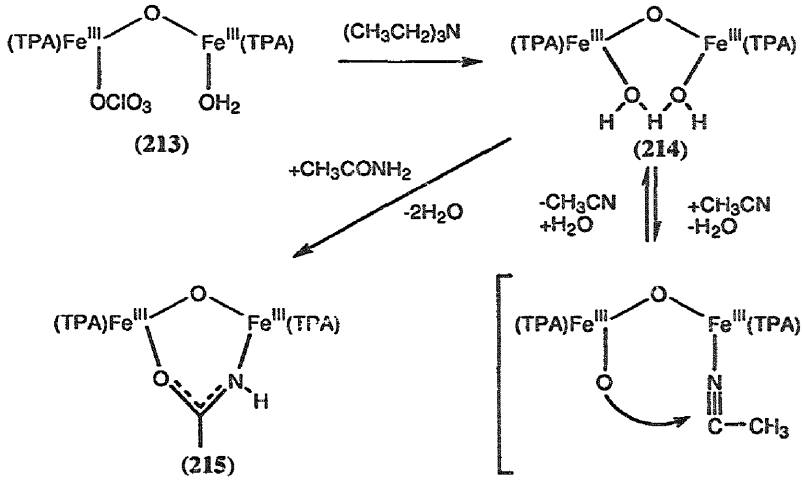

The diaqua-complex [(TPA)(H_2O)FeOFe(H_2O)(TPA)](ClO_4)$_4$ (**216**) is a good starting material for the preparation of new (μ-oxo)diiron(III) complexes. Displacement of the terminal ligand by chloro ligands gives [(TPA)(Cl)FeOFe(Cl)(TPA)](ClO_4)$_2$ (**217**) and replacement with a sulfato ligand gives the dibridged complex [(TPA)FeO(SO_4)Fe(TPA)](ClO_4)$_2$ [116]. The conjugate base of (**216**), [(TPA)(OH)FeOFe(H_2O)tpa](ClO_4)$_3$ (**218**) has also been prepared. The crystal structures of (**217**) and (**218**) have been determined. The structure of (**218**) shows that the hydroxo ligand and the terminal water are linked through an intramolecular hydrogen-bond and that the Fe-O(bridge) distances are unequal. Complex (**218**) promotes hydrolysis of acetonitrile to give the μ-acetamidato-N,O-bridged complex [(TPA)FeO(CH_3CONH)Fe(TPA)](ClO_4)$_3$ (**219**). All five complexes show a strong antiferromagnetic coupling. Electronic absorption and

resonance Raman measurements shows distinct differences between mono- and dibridged complexes.

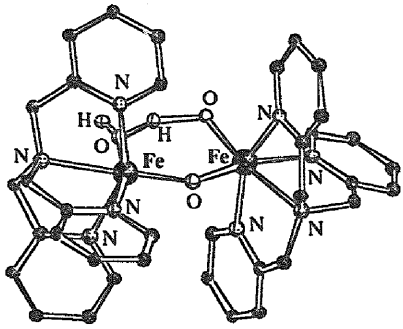

(218)

The dinuclear Fe(III) complexes $\{[(\mathbf{220})Fe]_2(\mu\text{-}O)(\mu\text{-}CO_3)\}(ClO_4)_2\cdot 3H_2O$ (**221**), $\{[(\mathbf{222})Fe]_2(\mu\text{-}O)(\mu\text{-}CO_3)\}(ClO_4)_2\cdot 2H_2O$ (**223**), $\{[(\mathbf{224})Fe]_2(\mu\text{-}O)(\mu\text{-}SO_4)\}(ClO_4)_2\cdot H_2O$ (**225**) and $\{[(\mathbf{220})Fe]_2(\mu\text{-}O)(\mu\text{-}SO_4)\}(ClO_4)_2\cdot 2H_2O$ (**226**) have been prepared and the crystal structures of (**221**), (**223**) and (**226**) have been determined [117]. Cyclic voltammetry reveals irreversible reduction peaks at -0.735 and -0.665 V *vs* Ag/AgCl for (**221**) and (**226**), respectively, while a *quasi*-reversible reduction at -0.585 V, corresponding to the $Fe_2(III/III)\leftrightarrow Fe_2(II/III)$ redox process, is observed for (**223**). Variable temperature magnetic measurements of (**223**) and (**226**) indicate that the two iron ions are antiferromagnetically coupled (**223**): $J=-105\ cm^{-1}$, (**226**): $J=-111\ cm^{-1}$.

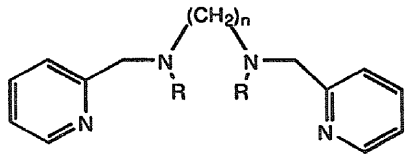

(**220**): n = 3, R = H, (**222**): n = 2, R = Me, (**224**): n = 2, R = H

Reaction of (**227**) with $Fe(NO_3)_3\cdot 9H_2O$ in methanol affords the compound $[Fe_2O(\mathbf{227})(CH_3OH)_5(H_2O)](NO_3)_2.4H_2O$ (**228**) whose structure has been determined by X-ray crystallography [118]. The crystal structure shows that the six solvent ligands are bound in terminal positions. Compound (**227**) reacts with *N*-donor ligands such as bpy to afford terminally substituted products, for example $[Fe_2O(\mathbf{227})(bpy)_2\text{-}(CH_3OH)_2]^{2+}$ (**229**). Stopped-flow kinetics analysis revealed the second order rate constant k to be $(1.51\pm 0.04)\times 10^3\ M^{-1}\ s^{-1}$, which is similar to observed kinetics for ligand substitution at a terminal site in hemerythrin. Various products of the general formula $[Fe^2O(XDK)(bpy)_2XY]^{n+}$ ($X=CH_3OH$, $Y=NO_3^-$, $n=1$; $X=Y=NO_3^-$, $n=0$, *anti*- and *syn*-forms) (**230**) were obtained from the reaction depending upon the isolation procedure used. Reaction of (**228**) with

1-methylimidazole resulted in successive replacement of each of the terminal solvent ligands, affording $[Fe_2O(\mathbf{227})(1\text{-MeIm})_6]^{2+}$ (**228**), the X-ray structure of which has been determined.

The Fe(III) to Fe(III) metal to metal charge transfer excitation of the Fe-O-Fe core has been studied in $[\{Fe^{III}(edta)\}_2O]^{4-}$ [119]. The reaction leads to disproportionation of iron yielding Fe^{II} and $Fe^{IV}=O$. Two oxoferryl fragments combine to generate Fe(II) and molecular oxygen. This system represents a simple model for photochemical oxidation of water or oxide.

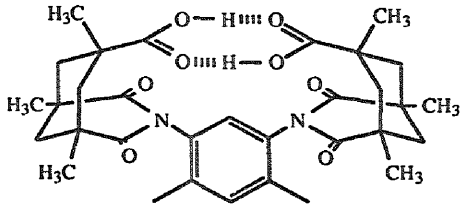

(227)

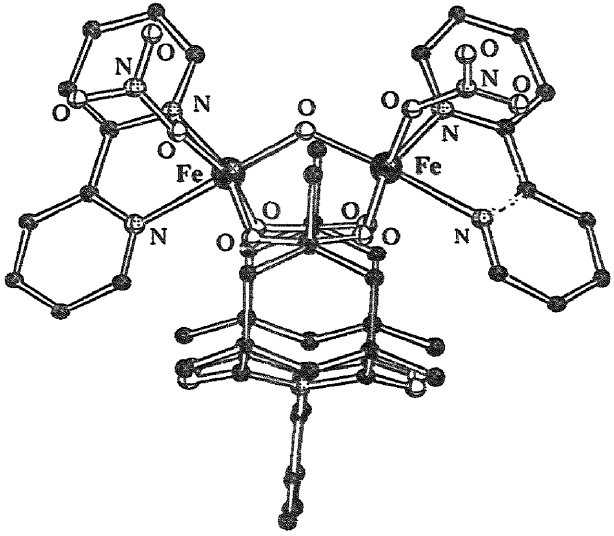

(230)

The combination of the phenolato-containing tripodal ligand (**231**), NEt_3, Na(bf) (bf = benzoylformate) and $Fe(ClO_4)_2 \cdot 6H_2O$ in methanol affords $[Fe(II)_2(\mathbf{231})_2(bf)]$-$(ClO_4)$ (**232**) [106]. The crystal structure of (**232**) shows that the two $Fe(II)_2$ centres are triply bridged by two phenolato ligands and the carboxylato group of the bf ligand. The Fe···Fe distance (3.049(2) Å) and Fe-O-Fe angle (93.2(2) and 91.6(2)°) are the smallest thus far reported for complexes with the

generalized $[Fe(II)_2(OR)_2]$ core. Exposure of an acetonitrile solution of (**232**) to air gives (**233**) and (**234**) in an equimolar amount. The mechanism shown below, which on the basis of spectroscopic analysis as well as isotopic experiments, is proposed to account for the observed reactivity. Upon exposure to dioxygen, the iron(II) complex (**232**) is stoichiometrically converted to a (μ-peroxo)diiron(III) complex. Intramolecular nucleophilic attack of the bound peroxide at the α-carbon of the bf ligand results in the oxidative decarboxylation of this α-ketoacid and the reduction of the peroxide to yield (**233**). Alternatively, this O_2 adduct can be reduced by a second molecule of (**232**) to afford the autoxidation product (**234**).

A variable-temperature infrared spectroscopic study on $[Fe(III)_2Fe(II)O(OOCMe)_6L_3]$ (L = py or d_5-py) has been carried out in order to measure rates of intramolecular electron transfer [120]. The bands assigned to in-plane vibration of the central oxygen atom show exceptional temperature dependence, interpreted as being due to electron transfer within the trinuclear cluster, with a rate constant of ca 10^{11} s^{-1} at 300 K.

As a biomimetic model of the active site in the hydroxylate protein of the methane monooxygenase enzyme a μ-oxo diiron complex, $[Fe_2O(H_2O)_2(235)_2](ClO_4)_4$ (**236**) has been synthesised and structurally characterized by X-ray crystallography [121]. The structure contains a bent Fe-O-Fe bridge with each iron atom also coordinated to the imidazole and amine nitrogen and a H_2O in a distorted octahedral. The complex catalyses the oxygenation of several hydrocarbons in the presence of H_2O_2 or *tert*-butyl hydroperoxide and dioxygen gas.

The complexes $[Fe_2(OH)(O_2CCH_3)_2(HBpz_3)_2](ClO_4)$ (**237**), $[Fe_2(OH)\{O_2P(OC_6H_5)_2\}_2(HBpz_3)_2](BF_4)$, and $[Fe_2(OH)\{O_2P(C_6H_5)_2\}_2(HBpz_3)_2](BF_4)$ have been prepared by protonation of their oxo-bridged analogues in ether solution [122]. Protonation of the oxo-bridges leads to expansion of the diiron core relative to the μ-oxo complexes; Fe-O and Fe···Fe distances as well Fe-O-Fe angles are larger. It also leads to a decrease in the antiferromagnetic spin exchange coupling. The complex $[Fe_2\{O_2P(OC_6H_5)_2\}_3(HBpz_3)_2](BF_4)$ (**238**), which contains three bridging groups, has also been synthesised and its structure determined by X-ray crystallography; the Fe-Fe distance in (**238**) is 4.677 Å.

The first example of a diferric complex with an oxo and a hydroxo bridge has been obtained from the reaction of one equivalent of FeX_2 (X = ClO_4 or CF_3SO_3) and (**239**) with five equivalents of ^{t}BuOOH in methanol/H_2O at -40°C [123]. It is proposed that the steric bulk of the methyl groups of ligand (**239**) prevents the ferric centre from making strong Fe-N bonds. This situation produces an Fe(III) ion with strong Lewis acidity, and in the absence of other potential ligands only hydroxy groups can lessen the high effective charge on the Fe(III). X-Ray crystallography shows that the iron atoms in the compound $[Fe_2O(OH)(239)_2](ClO_4)_3$ (**240**) have a distorted octahedral environment consisting of the four nitrogen atoms from (**239**) and two bridging oxygen atoms. The proposed structure is supported by EXAFS data. Incubation of (**240**) with 1-methyl-1,4-cyclohexadiene or PPh_3 leads to a reduced Fe(II) species, detected by sharp paramagnetically shifted signals in the NMR spectrum.

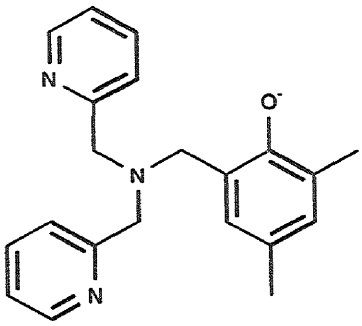

(231)

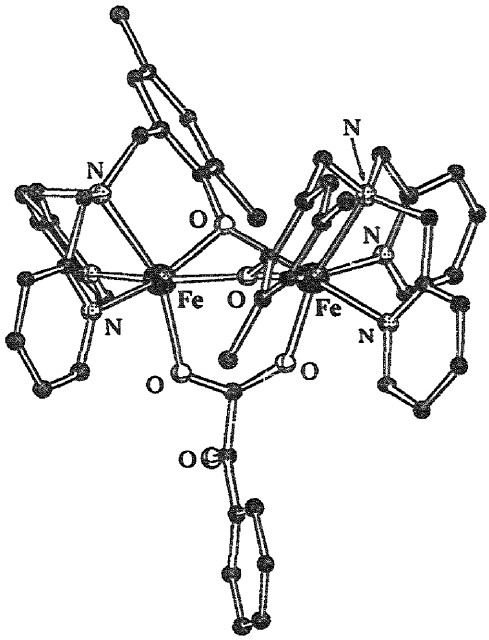

(232)

10.2. Polynuclear iron-oxo clusters

A molecular ferric wheel, $[Fe(OMe)_2(O_2CCH_2Cl)]_{10}$, has been synthesised from iron chloroacetate and ferric nitrate in methanol [124]. The X-ray crystal structure reveals a 20-membered ring comprising 10 ferric ions linked by 20 bridging methoxides and 10 bridging chloroacetate ligands. The 10 iron atoms are approximately coplanar, each forming a distorted octahedron with 6 oxygen donor atoms. From

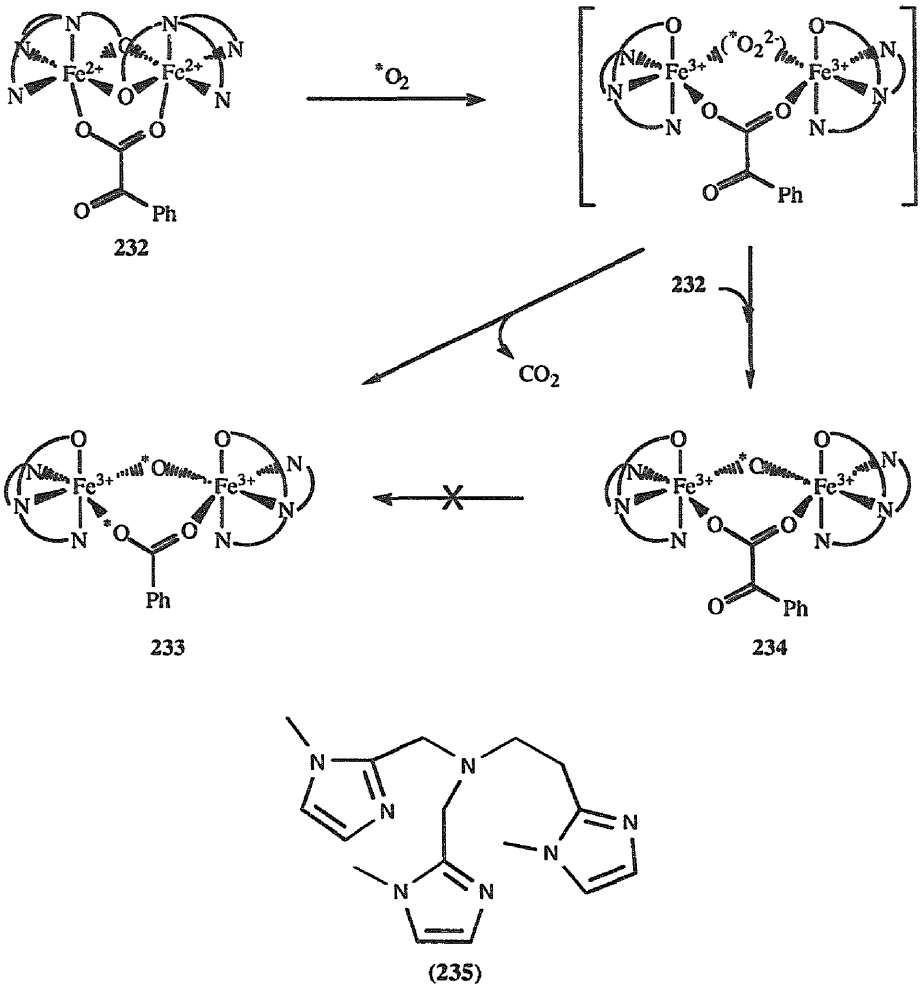

variable temperature magnetic studies a single antiferromagnetic exchange coupling constant J of 9.4 cm^{-1} was determined for nearest neighbour interactions. For this molecule S can adopt integer values from 0 to 25, revealed by field-dependent magnetic studies at 0.6 K.

A mixed-valent polyiron oxo complex has been synthesised as a model for the biomineralization of iron by ferritin. The complex, $[Fe(III)_4Fe(II)_8(O)_2(OMe)_{18}(OAc)_6(MeOH)_{4.67}]$ has also been structurally characterized by X-ray crystallography [125]. The structure consists of a face-centred cubic array of oxygen atoms with iron(II) and iron(III) ions in the octahedral interstices, the centre of the complex being two μ_6-oxo ligands. The mixed-valence nature was suggested based on Fe-O distances and electronic spectroscopy. Mössbauer spectro-

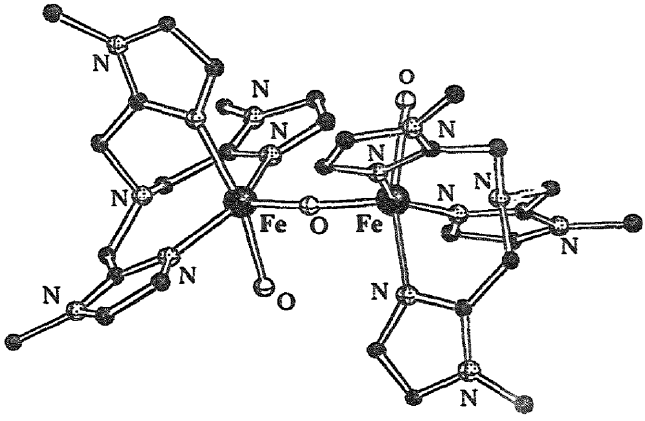

(236)

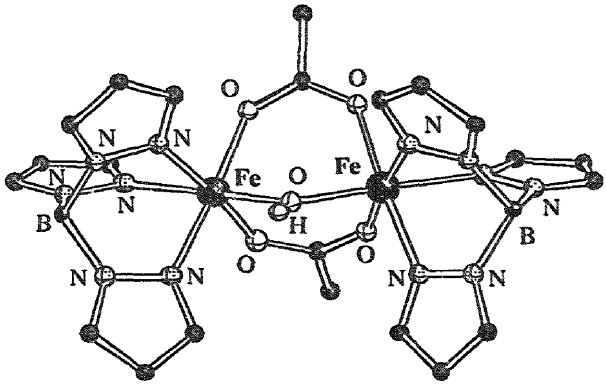

(237)

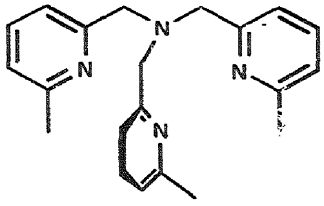

(239)

scopy reveals three distinguishable quadropolar doublets assigned as coming from iron(III) ions and two quadropolar doublets from iron(II) ions.

Magnetic susceptibility measurements on $[Fe_6O(\mathbf{241})_6](NMe_4)_2 \cdot 4CH_3OH$ [(**241**) =

the trianion of 1,1,1-tris(hydroxymethyl)ethane] and $Na_2[Fe_6O(OCH_3)_{18}]\cdot 6CH_3OH$, both of which contain $Fe(III)_6(\mu_6\text{-}O)$ cores, have been made [126]. X-Ray diffraction studies indicate that O_h symmetry is a fairly good description of the $Fe_6(\mu_6\text{-}O)$ cores. Therefore, only two kinds of exchange interactions need to be considered, the first involving *trans*-iron atoms (J_t) and the second involving *cis*-iron atoms (J_c). A very weak coupling between the metal centres in the $Fe_6(\mu_6\text{-}O)$ core was found ($J_t = 19(2)\,cm^{-1}$, $J_c = 9(1)\,cm^{-1}$). The lower value of J_c compared to J_t indicates that the relative contribution of ferromagnetic superexchange pathway mediated by the central O atom increases significantly as the Fe-O-Fe angle decreases from 180 to 90°.

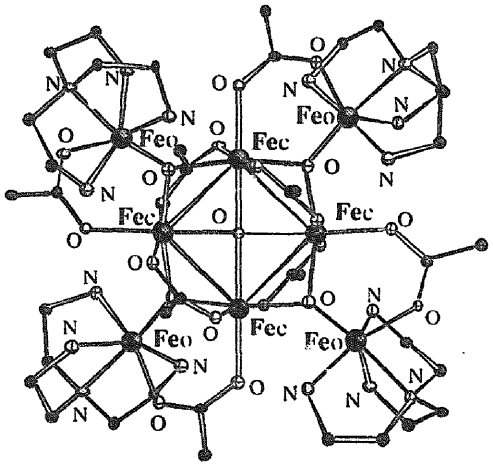

(242)

The structure of an iron(III)-oxo complex with a square-planar oxide has been reported [127] the complex is $[Fe_8(\mu_4\text{-}O)(\mu_3\text{-}O)_4(OAc)_8(tren)_4](CF_3SO_3)_6\cdot 5CH_3CN$ (**242**). The structure consists of an Fe_4O unit (labelled Fe_c) with four acetate ligands, each bridging two Fe_c atoms, two ligands above the Fe_4O plane and two below. Four other Fe atoms (Fe_o) are connected to the core by four μ_3-O ligands and four additional acetate ligands bridging one Fe_c and one Fe_o atom. The Fe_c atoms are coordinated to six oxygen atoms while the Fe_o atoms are connected to two oxygens and four nitrogens from the tren ligands. This structure is believed to be maintained in solution since the magnetic moments in the solid state and solution are similar.

The reaction of $FeCl_2$, R_2NH and CO_2 yields the iron(II) *N,N*-dialkylcarbamate complex $[\{Fe(O_2CNEt_2)_2\}_6]$ [128]. Controlled hydrolysis of the isopropyl derivative leads to $[\{Fe_4(\mu\text{-}O)(O_2CNPr^i_2)_6\}_2]$. This is the first example of an uncharged iron(II)-oxo complex.

10.3. Heterometallic iron-oxo clusters

The cluster $[Mn_8Fe_4O_{12}(O_2CMe)_{16}(H_2O)_4]\cdot 2MeCO_2H\cdot 4H_2O$ (**243**) has been synthesized by treatment of $Fe(O_2CMe)_2$ with $KMnO_4$ in 60% acetic acid followed by heating to 60°C [129]. An X-ray structure determination reveals that the molecule consists of a central $[Mn(IV)_4O_4]^{8+}$ cubane surrounded by a nonplanar eight-membered ring of alternating Mn(III) and Fe(III) ions. The ring and the cubane are held together by eight μ_3-O^{2-} ions. Electrochemical studies of (**243**) revealed one quasi-reversible reduction and one quasi-reversible oxidation. A comparison of the redox potentials for (**243**) to those of the related cluster $[Mn_{12}O_{12}(O_2CMe)_{16}(H_2O)_4]$ indicate that the reduction may take place at manganese centres. Magnetochemical and Mössbauer properties of (**243**) have been studied as well. ^{57}Fe Mössbauer spectra display two doublets, one corresponding to the four high spin Fe^{III} ions, the other doublets assigned to excess high spin Fe^{III} disordered throughout Mn^{III} sites. The effective magnetic moment (μ_{eff}) is 11.18 μ_B at 300 K decreasing to 4.85 μ_B at 5.00 K. This is dramatically different from the corresponding Mn_{12} cluster, thus replacing four Mn^{III} by four Fe^{III} ions dramatically affects the magnetochemistry. The Mn_4Mn_8 complex has a well isolated $S=2$ ground state compared to the $S=10$ ground state for the $Mn^{IV}_4Mn^{III}_8$ cluster.

Three polyiron complexes $[Fe_{16}MO_{10}(OH)_{10}(O_2CPh)_{20}]$, where M = Mn (**244**), Fe (**245**) or Co (**246**), have been synthesised from the triiron precursors $[Fe_3O(O_2PH)_6(H_2O)_2(MeCN)]$ and $[Fe_3O(O_2CPh)_6(Me_2O)_3](O_2CPh)$ [130]. The X-ray crystal structures of compounds (**244**) to (**246**) have been determined and in all cases the hetero-atom is located at the centre of symmetry. The polymetallic clusters can be formally constructed by fusion of two fragments of the previously reported compound $[Fe_{11}O_6(OH)_6(O_2CPh)_{15}]$. All the metal atoms have distorted octahedral geometry. Low temperature Mössbauer spectroscopic and magnetic studies reveal properties normally associated with solid-state infinite arrays.

The reaction of Tiron [where 1,2-dihydroxy-3,5-benzenesulfonate = (**247**)] with aqueous iron(III) has been studied by stopped flow spectrometry at moderate acidities (0.1-0.02 M H^+) [131]. A systematic variation of the bis(μ-hydroxo) dimer of iron(III) was made. At 660 nm there is a biphasic absorbance change. The faster increase in the absorbance is due to the reaction between $[(H_2O)_8Fe_2(\mu\text{-}OH)_2]^{4+}$ and Tiron. The reaction is pH-independent and gives a blue complex. This dimeric complex decomposes to $Fe(OH_2)_6^{3+}$ which is less strongly coloured and gives a slower decrease in absorbance.

11. Iron-sulfur clusters

11.1. Di- and trinuclear iron-sulfur clusters

The reaction of $Fe(II)Cl_2\cdot 4H_2O$ with 1,2-bis(2-mercaptophenylthio)ethane (**248**) yields the new iron-sulfur cluster [(μ-S_2){Fe(μ-**248**)}2] (**249**). Cluster (**249**) may also be prepared by the reaction of $Fe(PBu_3)_2$ (**248**) or $Fe(CO)_2$(**248**) with elemental

sulfur [132]. (**249**) contains *pseudo*-octahedral low-spin Fe centres coordinated by sulfur donors. Reaction of (**249**) with CO forms the known complex [{(CO)Fe(μ-**248**)}$_2$]. The crystal structure of (**249**) reveals that the cluster consists of two homochiral [FeL] fragments that are linked to each other via two thiolato donors and an S_2 bridge. The Fe-S distances of the FeS_2Fe moiety are unusually short (2.16 and 2.13 Å). Mössbauer spectroscopy indicates that the cluster contains two low-spin iron(II) centres. It is proposed that the FeS_2Fe unit of the comprises a 4c-6e system made up of the occupied Fe-d orbitals and the π and π* orbitals of the μ-S_2 ligand. Three absorptions within the UV-VIS-near-IR region at 640, 760 and 1050 nm are assigned to π-π transitions within the 4c-6e p system.

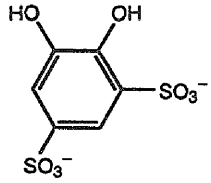

(**247**)

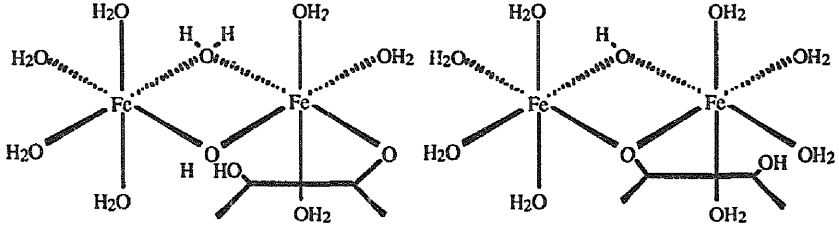

Proposed structures for the complex between $[(H_2O)_8Fe_2(OH)_4]^{4+}$ and (**247**). Only a part of the ligand is shown.

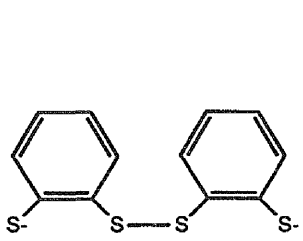

(**248**)

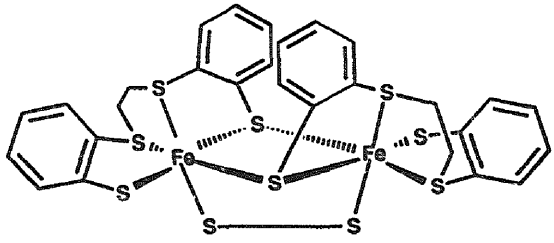

(**249**)

Kinetic studies on the substitution reactions of $[Fe_2S_2Cl_3(NCMe)]^-$ with the nucleophiles Br^-, EtS^-or $^tBuS^-$ to form $[Fe_2S_2Cl_3L]^{2-}$ show that the rate of the reaction is inhibited by increasing the concentration of the nucleophile [133]. This is a consequence of L binding to the iron atom not undergoing substitution.

11.2. Iron-sulfur cubanes

The reaction of $[Fe_4S_4X_4]^{2-}$ with excess isonitrile yields the clusters $[Fe_4S_4X_2(RNC)_6]$ (R = Me, t-Bu: X = halide), these can readily undergo substitution reactions at the halide sites to produce $[Fe_4S_4L_2(RNC)_6]$ (L = halide, RO^-, RS^-) [134]. Alternatively, thiolate clusters can be prepared from the reaction system $[Fe_4S_4(SR)_4]^{2-}/Et_3NH^+/RNC$.

The set of compounds $[Fe_4S_4L_2(RNC)_6]$ (L = halide, RO^-, RS^-) represents the largest and most thoroughly characterised [2:2] site-differentiated clusters, comprising two high-spin tetrahedral Fe(III) sites and two low-spin Fe(II) sites. X-Ray structural studies of the compounds $[Fe_4S_4L_2(t\text{-}BuNC)_6]$ [L = *p*-$MeC_6H_4O^-$ (**250**), PhS^- (**251**)] show the six-coordinate Fe(II) sites to be at non-bonding distances from each other and the two Fe(III) tetrahedral sites. The latter are implicated in an $[Fe_2S_2]^{2+}$ fragment very similar to the cores of the antiferromagnetically coupled clusters $[Fe_2S_2L_4]^{2-}$ [134]

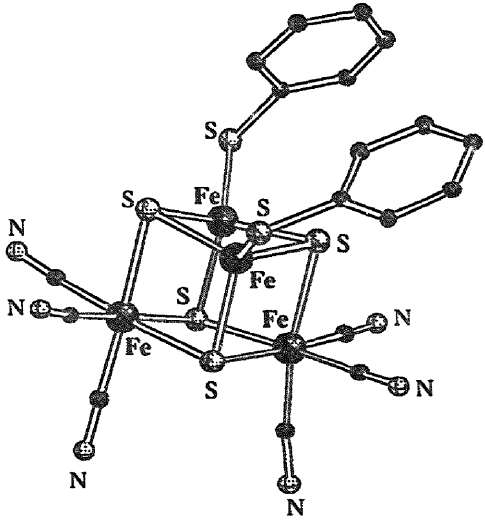

(251)

Two classes of enzyme, hydrogenases and nitrogenases evolve hydrogen by the reduction of protons. The precursor in this process is assumed to be a hydridic species although no evidence has been obtained. However, protonation of the iron sulfur core at the $\{Fe_4S_4\}^{2+}$ redox level in $[Fe_4S_4X_4]^{2-}$ (X = Cl or Br) has provided the first chemical conformation for this biochemical reaction [135].

EPR Spectroscopic studies of γ-irradiated single crystals of $[Et_4N]_2[Fe_4S_4(SCH_2C_6H_5)_4]$ and its partially and fully deuterated counterparts reveal five $[Fe_4S_4]^{3+}$ paramagnetic species, corresponding to the oxidised state of the high-potential proteins and two $[Fe_4S_4]^+$ species corresponding to the reduced

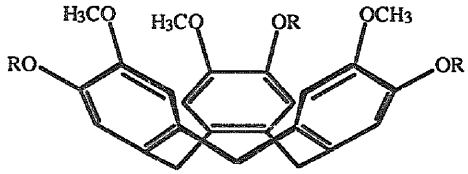

(252): R = CH_2CH_2SH; (253): R = *m*-$CH_2C_6H_4CH_2SH$

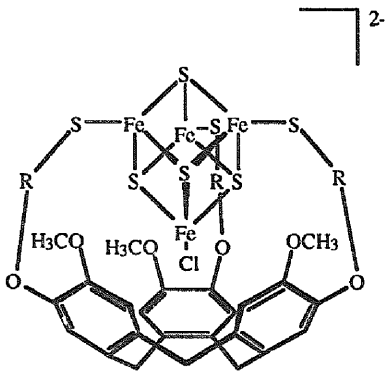

(254): R = -CH_2CH_2-; (255): R = -$CH_2C_6H_4S$-

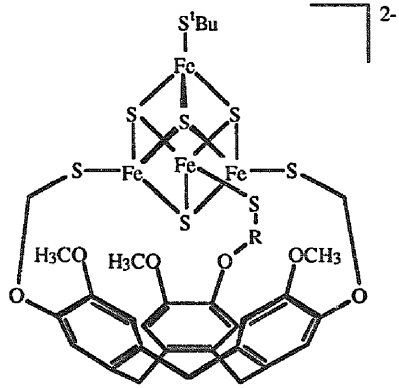

(256): R = -CH_2CH_2-;
(257): R = -$CH_2C_6H_4S$-

state of the ferredoxins. The results obtained on the $[Fe_4S_4]^+$ state suggest a new interpretation of the composite EPR spectrum of the oxidised high potential *Chromatium vinosum* protein [136].

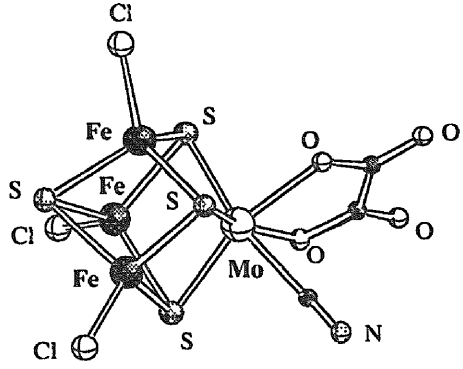

(259)

Density functional calculations for 1Fe, 2Fe and 4Fe iron-sulfur clusters showing a good correlation between predicted and measured redox potentials have been carried out [137]. The effect of the solvent was modelled through a continuum

dielectric and was found to be large in all clusters and redox couples. The calculations suggest that the solvent mainly compensates for differences in electron-electron repulsion energies in vacuum. For the 4Fe high potential clusters, three low-lying electronic states where found suggesting that the situation in synthetic models and proteins could involve any of these three states.

Reaction of the trithiol ligands (**252**) and (**253**) which are based on the bowl-like building block cyclotriveratrylene with $[Fe_4S_4Cl_4]^{2-}$ in the presence of base gives the subsite-differentiated clusters $[(\mathbf{252})Fe_4S_4Cl]^{2-}$ (**254**) and $[(\mathbf{253})Fe_4S_4Cl]^{2-}$ (**255**) with the cluster core partially encapsulated and the subsite oriented inwards [138]. If $[Fe_4S_4(S^tBu)_4]^{2-}$ is reacted with (**252**) or (**253**), the products are the *tert*-butylthiol derivatives of (**252**) and (**253**) ((**256**) and (**257**), respectively) and here the subsite is oriented outwards.

11.3. Heterometallic iron-sulfur clusters

The reaction of $(Et_4N)_3[(C_2O_4)MoFe_3S_4Cl_4]$ (**258**) with $(Et_4N)CN$ affords $[(C_2O_4)(CN)MoFe_3S_4Cl_3]^{3-}$ (**259**) in nearly quantitative yields [139]. The reaction of (**258**) with 0.5 eq. of $(Et_4N)CN$ and 0.5 equivalents of a source of S^{2-} affords the doubly-bridged double-cubane $\{[(C_2O_4)MoFe_3S_4Cl_2]_2(\mu_2\text{-}CN)(\mu_2\text{-}S)\}^{5-}$ (**260**) in 30% yield. Single crystal X-ray structures were determined for (**259**) and (**260**). The mean Fe-Fe, Fe-S and Fe-Cl bond distances in (**259**) at 2.713(3), 2.270(5) and 2.214(5) Å, are typical for $MoFe_3S_4$ cubane-like structures.

The penta-anion (**260**) consists of two doubly-bridged cubane subunits bridged by a μ_2-CN^- ligand through the Mo atoms and a μ_2-S^{2-} through two Fe atoms. The Mo···Mo and Fe···Fe(intercube) distances and the Fe-μ_2-S-Fe angle are found at 5.267(4), 3.443(7) and 104.1(4)°. The cyclic voltammetry of **2** (on a Pt working electrode, in CH_2Cl_2, *vs* Ag/AgCl) shows a single reduction (-1090 mV) and oxidation (+330 mV). In contrast, (**260**) shows multiple reductions (-1110 mV, -1500 mV) and oxidations (+50 mV, +300 mV). The doubling of the voltammetric waves in (**260**) with appreciable differences in redox potentials suggests that the double-cubane structure is retained in solution and indicates significant electronic communication between the two cuboidal subunits. The lack of an EPR signal in solutions of (**260**) also indicates electronic communication and effective spin coupling between the $S=3/2$ subunits.

Improved preparations of the heterometal clusters $MFe_4S_6(PEt_3)_4Cl$ [M=V(**261**), Mo(**262**)] are reported [140]. Reaction of these clusters with NaSR yields the compounds $MFe_4S_6(PEt_3)_4(SR)$ [M=V, R=Ph (**263**); R=Et (**264**); M=Mo, R=Ph (**265**); R=Et (**266**)]. The crystal structures of compounds (**263**) and (**265**) have been determined. The thiolate ligand has been shown to bind at the axial site forming tetrahedral $FeS_3(SR)$ units. The additional valence electron in the molybdenum clusters is believed to be largely delocalised in the Fe_4S_3 cuboidal portion. Cluster (**261**) exhibits the first example of a spin state equilibrium ($S=0\leftrightarrow S=1$) in any iron-sulphur cluster, whereas clusters (**262**) and (**265**) have $S=1/2$ or spin-admixed ($S=1/2$, 3/2) ground states.

A novel synthetic pathway to hexacapped mixed-metal cubic $[M_8S_6]$ clusters has been found [141]. Reactions of the easily accessible $[Fe_4S_4I_4]^{2-}$ with appropriate

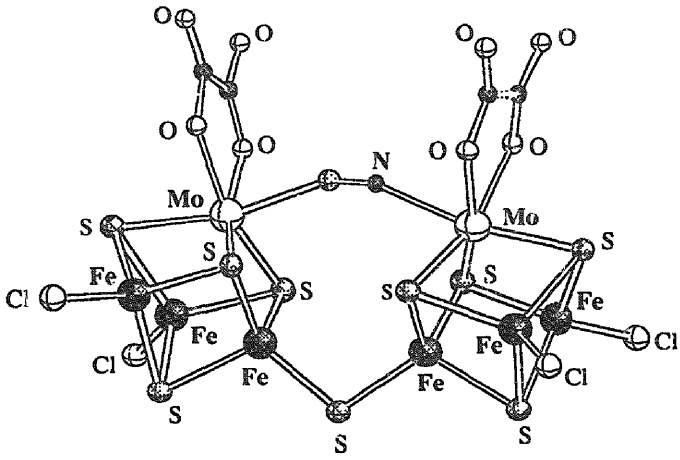

(260)

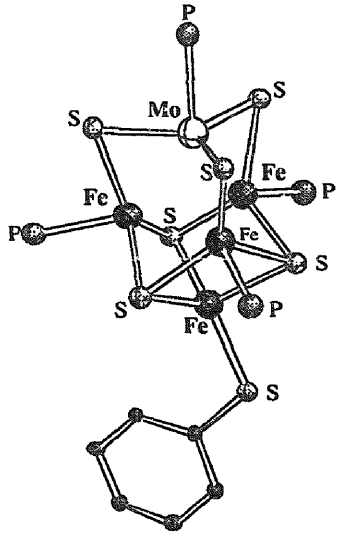

(265)

mononuclear complexes and phosphines or with phosphine-coordinated complexes give $[Fe_{8-x}M_xS_6]$ clusters (x = 1-4). The isolation and characterisation by single-crystal X-ray crystallography of $[PhCH_2NEt_3]_2[Fe_6Ni_2S_6I_6(PMePh_2)_2]$ and $[Fe_4Ni_4S_6I_4(PMePh_2)_4]$ have been reported.

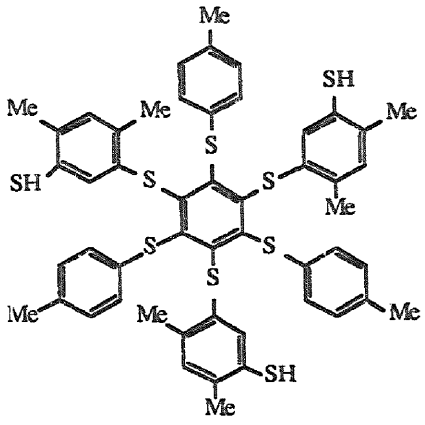

(266)

11.4. Other iron-sulfur clusters

The reaction of $[Fe_4S_4(\mathbf{266})(SEt)]^{2-}$ with limited H_2S affords the functionalised cluster $[Fe_4S_4(\mathbf{266})(SH)]^{2-}$ (**267**) which exists in equilibrium with the μ-S_2 double cubane $\{[Fe_4S_4(\mathbf{266})]_2S_2\}^{4-}$ and H_2S [142]. Reaction of (**267**) and $[Fe(salen)]_2O$ yielded the bridged assembly $[Fe_4S_4(\mathbf{266})-S-Fe(III)(salen)]^{2-}$ (**268**). The compound $[Fe_4S_4(\mathbf{266})-S-Fe(III)(OEP)]^{2-}$ (**269**) can be prepared by six different reactions: Direct coupling of cluster (**267**) with $[Fe(OEP)_2]O$, [Fe(OEP)(OMe)], $[Fe(OEP=(OC(Me)=CH_2)]$, and $[Fe(OEP)(OClO_3)]/Et_3N$; Si-S bond cleavage in the reaction of $[Fe_4S_4(\mathbf{266})(SSiEt_3)]^{2-}$ with [Fe(OEP)F]; and oxidative addition of [Fe(II)(OEP)] to the disulfide bond of the μ-S_2 double cubane $\{[Fe_4S_4(\mathbf{266})]_2S_2\}^{4-}$. Isotropic shifts in the ^1H NMR spectra originate from extensive spin localization from the Fe(III) fragments to the cluster. Compounds (**268**) and (**269**) sustain two one-electron reduction reactions; other reactions of (**269**) which alter or cleave the bridge are also summarised.

Acknowledgements

We thank Maria Johansson and Roger Persson for assistance in the bibliographic research.

References

[1] R.H. Morris and M. Schlaf, Inorg. Chem., 33 (1994) 1725.
[2] G. Albertin, S. Antoniutti, E. Del Ministro and E. Bordignon, J. Chem. Soc., Dalton Trans., (1994) 1769.

[3] M.T. Bautista, K.A. Earl, P.A. Maltby and R.H. Morris and C.T. Schweitzer, Can. J. Chem., 72 (1994) 547.
[4] S.S. Borges, A.L. Coelho, I.C. Moreira and M.A.B. de Araujo, Polyhedron, 13 (1994) 1015.
[5] C. Roux, J. Zarembowitch, B. Gallois, T. Granier and R. Claude, Inorg. Chem., 33 (1994) 2273.
[6] N. Arulsamy, J. Glerup and D.J. Hodgson, Inorg. Chem., 33 (1994) 3043.
[7] M. Goto, N. Koga, Y. Ohse, H. Kurosaki, T. Komatsu and Y. Kuroda, J. Chem. Soc., Chem. Commun., (1994) 2015.
[8] N. Arulsamy and D.J. Hodgson, Inorg. Chem., 33 (1994) 4531.
[9] A.K. Tripathi, P. Mathur and J.S. Baijal, Polyhedron, 13 (1994) 1005.
[10] J.L. Sessler, J.W. Sibert and V. Lynch, Inorg. Chim. Acta, 216 (1994) 89.
[11] M. Di Vaira, F. Mani and P. Stoppioni, J. Chem. Soc., Dalton Trans., (1994) 3739.
[12] N. Kitajima, N. Tamura, H. Amagai, H. Fukui, Y. Morooka, Y. Mizutani, T. Kitagawa, R. Mathur, K. Heerwegh, C.A. Reed, C.R. Randall, L. Que and K. Tatsumi, J. Am. Chem. Soc., 116 (1994) 9071.
[13] M. Thomann, O. Kahn, J. Guilhem and F. Varret, Inorg. Chem., 33 (1994) 6029.
[14] J.P. Martin, J. Zarembowitch, A. Dworkin, J.G Haasnoot and E. Codjovi, Inorg. Chem., 33 (1994) 2617.
[15] J.P. Martin, J. Zarembowitch, A. Bousseksou, A. Dworlin, J.G. Haasnoot and F. Varret, Inorg. Chem., 33 (1994) 6325.
[16] J.A. Real, M.C. Munoz, E. Andres, T. Granier and B. Gallois, Inorg. Chem., 33 (1994) 3587.
[17] F.A. Cotton, L.M. Daniels and C.A. Murillo, Inorg. Chim. Acta, 224 (1994) 5.
[18] F.A. Cotton, L.M. Daniels, L.R. Falvello and C.A. Murillo, Inorg. Chim. Acta, 219 (1994) 7.
[19] M. Shakir, S.P. Varkey, F. Firdaus and P.S. Hameed, Polyhedron, 13 (1994) 2319.
[20] L.L. Martin, R.L. Martin and A.M. Sargeson, Polyhedron, 13 (1994) 1969.
[21] H.S. Mountford, D.B. Macqueen, A.P. Li, J.W. Otvos, M. Calvin, R.B. Frankel and L.O. Spreer, Inorg. Chem., 33 (1994) 1748.
[22] L.O. Spreer, A.P. Li, D.B. Macqueen, C.B. Allan, J.W. Otvos, M. Calvin, R.B. Frankel and G.C. Papaefthymiou, Inorg. Chem., 33 (1994) 1753.
[23] D.V. Stynes, Inorg. Chem., 33 (1994) 5022.
[24] S.D. Christie, S. Subramanian, L.K. Thompson and M.J. Zaworotko, J. Chem. Soc., Chem. Commun., (1994) 2563.
[25] W. Linert, M. Konecny and F. Renz, J. Chem. Soc., Dalton Trans., (1994) 1523.
[26] T. Buchen, P. Gutlich and H.A. Goodwin, Inorg. Chem., 33 (1994) 4573.
[27] R.J. Guajardo, J.D. Tan and P.D. Mascharak, Inorg. Chem., 33 (1994) 2838.
[28] C.C. Cummins and R.R. Schrock, Inorg. Chem., 33 (1994) 395.
[29] E.A. Ough and M.J. Stillman, Inorg. Chem., 33 (1994) 573.
[30] K. Suda, M. Sashima, M. Izutsu and F. Hino, J. Chem. Soc., Chem. Commun., (1994) 949.
[31] I. Bhugun, D. Lexa and J.-M. Saveant, J. Am. Chem. Soc., 116 (1994) 5015.
[32] L. Weber, R. Hommel, J. Behling, G. Haufe and H. Hennig, J. Am. Chem. Soc., 116 (1994) 2400.
[33] S. Sakaki, T. Kimura, T. Ogata, H. Hasuo and T. Arai, New J. Chem., 18 (1994) 231.
[34] K.M. Kadish, F. D'Souza, A. Villard, M. Autret, E. Van Caemelbecke, P. Bianco, A. Antonini and P. Tagliatesta, Inorg. Chem., 33 (1994) 5169.
[35] D. Mansuy, Pure Appl. Chem., 66 (1994) 737.
[36] M.W. Grinstaff, M.G. Hill, J.A. Labinger and H.B. Gray, Science, 264 (1994) 1311.
[37] M.K. Safo, F.A. Walker, A.M. Raitsimring, W.P. Walters, D.P. Dolata, P.G. Debrunner and W.R. Scheidt, J. Am. Chem. Soc., 116 (1994) 7760.
[38] Y. Zhang, W.A. Hallows, W.J. Ryan, J.G. Jones, G.B. Carpenter and D.A. Sweigart, Inorg. Chem., 33 (1994) 3306.
[39] H. Tan, U. Simonis, N.V. Shokhirev and F.A. Walker, J. Am. Chem. Soc., 116 (1994) 5784.
[40] M. Nakamura, K. Tajima, K. Tada, K. Ishizu and N. Nakamura, Inorg. Chim. Acta, 224 (1994) 113.
[41] J.A. Gonzalez and L.J. Wilson, Inorg. Chem., 33 (1994) 1543.
[42] Y. Iamamoto, K.J. Ciuffi, H.C. Sacco, C.M.C. Prado, M. de Moraes and O.R. Nascimento, J. Mol. Catal., 88 (1994) 167.
[43] B. Cheng, M.K. Safo, R.D. Orosz, C.A. Reed, P.G. Debrunner and W.R. Scheidt, Inorg. Chem., 33 (1994) 1319.

[44] A. Maldotti, C. Bartocci, R. Amadelli, G. Varani and M.C. Pietrogrande, Gazz. Chim. Ital., 124 (1994) 411.
[45] A. Ghosh, J. Almlof and L.J. Que, J. Phys. Chem., 98 (1994) 5576.
[46] H. Fuji, Chem. Lett., 8 (1994) 1491.
[47] J.T. Groves, Z. Gross and M.K. Stern, Inorg. Chem., 33 (1994) 5065.
[48] M. Muether, E. Bill, A.X. Trautwein, D. Mandon, R. Weiss, A. Gold, K. Jayaraj and R.N. Austin, Hyperfine Interact, 91 (1994) 803.
[49] Z. Gross and S. Nimri, Inorg. Chem., 33 (1994) 1731.
[50] P.E. Ellis, J.E. Lyons and S.N. Shaikh, Catalysis Lett., 24 (1994) 79.
[51] H.R. Jimenez, J.M. Moratal, J. Faus and M. Momenteau, New J. Chem., 18 (1994) 1247.
[52] S. David, B.R. James, D. Dolphin, T.G. Traylor and M.A. Lopez, J. Am. Chem. Soc., 116 (1994) 6.
[53] H.R. Jimenez and M. Momenteau, New J. Chem., 18 (1994) 569.
[54] C. Tetreau, D. Lavalette, M. Momenteau, J. Fischer and R. Weiss, J. Am. Chem. Soc., 116 (1994) 11840.
[55] M. Ravikanth, A. Misra, D. Reddy and T.K. Chandrashekar, J. Chem. Soc., Dalton Trans., (1994) 491.
[56] J.P. Collman, X. Zhang, K. Wong and J.I. Brauman, J. Am. Chem. Soc., 116 (1994) 6245.
[57] G.B. Ray, X.Y. Li, J.A. Ibers, J.L. Sessler and T.G. Spiro, J. Am. Chem. Soc., 116 (1994) 162.
[58] N. Kobayashi, K. Mizuno and T. Osa, Inorg. Chim. Acta, 224 (1994) 1.
[59] G. Balducci, G. Chottard, C. Gueutin, D. Lexa and J.-M. Saveant, Inorg. Chem., 33 (1994) 1972.
[60] E. Anxolabehere, G. Chottard and D. Lexa, New J. Chem., 18 (1994) 889.
[61] Y. Mizutani, Y. Watanabe and T. Kitagawa, J. Am. Chem. Soc., 116 (1994) 3439.
[62] Z. Gryczynski, R. Paolesse, K.M. Smith and E. Bucci, J. Phys. Chem., 98 (1994) 8813.
[63] C.E. Castro and E.W. Bartnicki, J. Org. Chem., 59 (1994) 4051.
[64] S. Wolowiec and L. Latos-Grazynski,. Inorg. Chem., 33 (1994) 3576.
[65] S. Yoshinori, N. Sawada and M. Tadokoro, Chem. Lett., 9 (1994) 1713.
[66] B. Song and H.M. Goff, Inorg. Chem., 33 (1994) 5979.
[67] T. La, R. Richards and G.M. Miskelly, Inorg. Chem., 33 (1994) 3159.
[68] J.F. Bartoli, P. Battioni, W.R. De Foor and D. Mansuy, J. Chem. Soc., Chem. Commun., (1994) 23.
[69] P. Basu, A.M. Raitsimring, M.J. LaBarre, I.K. Dhawan, J.L. Weibrecht and J.H.J. Enemark, J. Am. Chem. Soc., 116 (1994) 7166.
[70] S.F. Huang and H.H. Wei, Hyperfine Interact, 91 (1994) 809.
[71] K.D. Karlin, A. Nanthakumar, S. Fox, N.N. Murphy, N. Ravi, B.H. Huynh, R.D. Orosz and E.P. Day, J. Am. Chem. Soc., 116 (1994) 4753.
[72] M.J. Scott and R.H. Holm, J. Am. Chem. Soc., 116 (1994) 11357.
[73] S.C. Lee, M.J. Scott, K. Kauffmann, E. Munck and R.H. Holm, J. Am. Chem. Soc., 116 (1994) 401.
[74] S. Ozawa, Y. Watanabe, S. Nakashima, T. Kitagawa and I. Morishima, J. Am. Chem. Soc., 116 (1994) 634.
[75] S. Ozawa, Y. Watanabe and I. Morishima, Inorg. Chem., 33 (1994) 306.
[76] S. Ozawa, E. Sakamoto, Y. Watanabe and I. Morishima, J. Chem. Soc., Chem. Commun., (1994) 935.
[77] S. Ozawa, Y. Watanabe and I. Morishima, J. Am. Chem. Soc., 116 (1994) 5832.
[78] M. Autret, S. Will, E. Vancaemelbecke, J. Lex, J.P. Gisselbrecht, M. Gross, E. Vogel and K.M. Kadish, J. Am. Chem. Soc., 116 (1994) 9141.
[79] K.M. Kadish, P. Boulas, F. D'Souza, M.A. Aukauloo, R. Guilard, M. Lausmann and E. Vogel, Inorg. Chem., 33 (1994) 471.
[80] C. Bernard, J.P. Gisselbrecht, M. Gross, E. Vogel and M. Lausmann, Inorg. Chem., 33 (1994) 2393.
[81] R.F. Saalfrank, R. Burak, A. Breit, D. Stalke, R. Herbst-Irmer, J. Daub, M. Porsch, E. Bill, M. Muther and A.X. Trautwein, Angew. Chem., Int. Ed. Engl., 33 (1994) 1621.
[82] G.M. Escandar, A.C. Olivieri, M. Gonzales-Sierra and L.F. Sala, J. Chem. Soc., Dalton Trans., (1994) 1189.
[83] I. Shweky, A. Bino, D.P. Goldberg and S.J. Lippard, Inorg. Chem. 33 (1994) 5161.
[84] C. Mathoniere, S.G. Carling, Y. Dou and P. Day, J. Chem. Soc., Chem. Commun., (1994) 1551.
[85] S. Decurtins, H.W. Schmalle, P. Schneuwly, J. Ensling and P. Gütlich, J. Am. Chem. Soc., 116 (1994) 9521.

[86] M.T. Caudle, R.D. Stevens and A.L. Crumbliss, Inorg. Chem., 33 (1994) 6111.
[87] M.T. Caudle, L.P. Cogswell and A.L. Crumbliss, Inorg. Chem., 33 (1994) 4759.
[88] M.T. Caudle and A.L. Crumbliss, Inorg. Chem., 33 (1994) 4077.
[89] M.T. Caudle, R.D. Stevens and A.L. Crumbliss, Inorg. Chem., 33 (1994) 843.
[90] V. Munyejabo, P. Guillaume and M. Postel, Inorg. Chim. Acta, 221 (1994) 133.
[91] A.J. Blake, R.O. Gould, C.M. Grant, P.E.Y. Milne and R.E.P. Winpenny, Polyhedron, 13 (1994) 187.
[92] Z.G. Hou, D.W. Whisehunt, J.D. Xu and K.N. Raymond, J. Am. Chem. Soc., 116 (1994) 840.
[93] J. Suh, S.H. Lee and H.J. Paik, Inorg. Chem., 33 (1994) 3.
[94] M. Albrecht, S.J. Franklin and K.N. Raymond, Inorg. Chem., 33 (1994) 5785.
[95] T. Funabiki, M. Ishikawa, Y. Nagai, J. Yorita and S. Yoshida, J. Chem. Soc., Chem. Commun., (1994) 1951.
[96] A.S. Attia, O.-S. Jung and C.G. Pierpont, Inorg. Chim. Acta, 226 (1994) 91.
[97] M.E. Bodini, P.E. Bravo and M.V. Arancibia, Polyhedron, 13 (1994) 497.
[98] J.F. Ellison, K. Ruhlandt-Senge and P.P. Power, Angew. Chem., Int. Ed. Engl., 33 (1994) 1178.
[99] R.S. Czernuszewicz, L.K. Kilpatrick, S.A. Koch and T.G. Spiro, J. Am. Chem. Soc., 116 (1994) 7134.
[100] D. Sellmann, T. Hofmann, and F. Knoch, Inorg. Chim. Acta, 224 (1994) 61.
[101] D. Sellmann, T. Becker, T. Hofmann, F. Knoch and M. Moll, Inorg. Chim. Acta, 219 (1994) 75.
[102] N.R. Champness, W. Levason, R.D. Oldroyd and S.R. Preece, Inorg. Chem., 33 (1994) 2060.
[103] D. Boinnard, A. Bousseksou, A. Dworkin, J.M. Savariault, F. Varret and J.P. Tuchagues, Inorg. Chem., 33 (1994) 271.
[104] J.E. Bollinger, J.T. Mague and D.M. Roundhill, Inorg. Chem., 33 (1994) 1241.
[105] B. Krebs, K. Schepers, B. Bremer, G. Henkel, E. Althaus, W. Mullerwarmuth, K. Griesar and W. Haase, Inorg. Chem., 33 (1994) 1907.
[106] Y.-M. Chiou and L. Que Jr., Angew. Chem., Int. Ed. Engl., 33 (1994) 1886.
[107] S. Sandiurena and E.J. Parsons, Inorg. Chem., 33 (1994) 302.
[108] A.M. Whalen, S. Bhattacharya and C.G. Pierpont, Inorg. Chem., 33 (1994) 347.
[109] C. Kang, A. Sobkowiak and D.T. Sawyer, Inorg. Chem., 33 (1994) 79.
[110] W.K. Lin, W.J. Welsh and W.R. Harris, Inorg. Chem., 33 (1994) 884.
[111] A.L. Feig and S.J. Lippard, J. Am. Chem. Soc., 116 (1994) 8410.
[112] M.P. Hendrich, E.P. Day, C.P. Wang, B.S. Snyder, R.H. Holm and E. Munck, Inorg. Chem., 33 (1994) 2848.
[113] E. Konig, G. Ritter, H. Grunsteudel, J. Dengler and J. Nelson, Inorg. Chem., 33 (1994) 837.
[114] P. Chakraborty, S.K. Chandra and A. Chakravorty, Inorg. Chem., 33 (1994) 6429.
[115] E.C. Wilkinson, Y. Dong and L. Que, J. Am. Chem. Soc., 116 (1994) 8394.
[116] A. Hazell, K.B. Jensen, C.J. McKenzie and H. Toftlund, Inorg. Chem., 33 (1994) 3127.
[117] N. Arulsamy, P.A. Goodson, D.J. Hodgson, J. Glerup and K. Michelsen, Inorg. Chim. Acta, 216 (1994) 21.
[118] S.P. Watton, A. Masschelein, J. Rebek and S.J. Lippard, J. Am. Chem. Soc., 116 (1994) 5196.
[119] H. Kunkely and A. Vogler, J. Chem. Soc., Chem. Commun., (1994) 2671.
[120] R. Wu, S.K.A. Koske, R.P. White, C.E. Anson, U.A. Jayasooriya and R.D. Cannon, J. Chem. Soc., Chem. Commun., (1994) 1657.
[121] R.M. Buchanan, S. Chen, J.F. Richardson, M. Bressan, L. Forti, A. Morvillo and R.H. Fish, Inorg. Chem., 33 (1994) 3208.
[122] P.N. Turowski, W.H. Armstrong, S.C. Liu, S.N. Brown and S.J. Lippard, Inorg. Chem., 33 (1994) 636.
[123] Y. Zang, G.F. Pan, L. Que, B.G. Fox and E. Munck, J. Am. Chem. Soc., 116 (1994) 3653.
[124] K.L. Taft, C.D. Delfs, G.C. Papaefthymiou, S. Foner, D. Gatteschi and S.J. Lippard, J. Am. Chem. Soc., 116 (1994) 823.
[125] K.L. Taft, G.C. Papaefthymiou and S.J. Lippard, Inorg. Chem., 33 (1994) 1510.
[126] A. Cornia, D. Gatteschi and K. Hegetschweiler, Inorg. Chem., 33 (1994) 1559.
[127] V.S. Nair and K.S. Hagen, Inorg. Chem., 33 (1994) 185.
[128] D. Belli Dell'Amico, F. Calderazzo, L. Labella, C. Maichle-Moessmer and J. Straehle, J. Chem. Soc., Chem. Commun., (1994) 1555.

[129] A.R. Schake, H.L. Tsai, R.L. Webb, K. Folting, G. Christou and D.N. Hendrickson, Inorg. Chem., 33 (1994) 6020.
[130] W. Micklitz, V. McKee, R.L. Rardin, L.E. Pence, G.C. Papaefthymiou, S.G. Bott and S.J. Lippard, J. Am. Chem. Soc., 116 (1994) 8061.
[131] J. Chatlas and R.B. Jordan, Inorg. Chem., 33 (1994) 3817.
[132] D. Sellmann, G. Mahr, and F. Knoch, Inorg. Chim. Acta, 224 (1994) 35.
[133] R.A. Henderson and K.E. Oglieve, J. Chem. Soc., Chem. Commun., (1994) 1961.
[134] C. Goh, J.A. Weigel and R.H. Holm, Inorg. Chem., 33 (1994) 4861.
[135] R.A. Henderson and K.E. Oglieve, J. Chem. Soc., Chem. Commun., (1994) 377.
[136] J. Gloux, P. Gloux, B. Lamotte, J.M. Mouesca and G. Rius, J. Am. Chem. Soc., 116 (1994) 1953.
[137] J.-M. Mouesca, J.L. Chen, L. Noodleman, D. Bashford and D.A. Case, J. Am. Chem. Soc., 116 (1994) 11898.
[138] G.P.F. Vanstrijdonck, J.A.E.H. Vanhaare, J.G.M. Vanderlinden, J.J. Steggerda and R.J.M. Nolte, Inorg. Chem., 33 (1994) 999.
[139] K.D. Demadis, S.-J. Chen and D. Coucouvanis, Polyhedron, 13 (1994) 3147.
[140] W. Cen, F.M. MacDonnell, M.J. Scott and R.H. Holm, Inorg. Chem., 33 (1994) 5809.
[141] C. Junghans, W. Saak and S. Pohl, J. Chem. Soc., Chem. Commun., (1994) 2327.
[142] L.S. Cai and R.H. Holm, J. Am. Chem. Soc., 116 (1994) 7177.
[143] E. Bernard, W. Moneta, J. Laugier, S. Chardon-Nobalt, A. Deronzier, J.-P. Tuchagues, and J.M. Latour, Angew. Chem., Int. Ed. Engl., 33 (1994) 887.